

**Facile Hydrothermal Synthesis of Nickel
Manganese Oxide/Activated Carbon
nanowires as electrode material for
Supercapacitors**



By

Faiza Khalid

**School of Chemical and Material Engineering
National University of Sciences and Technology**

2020

Facile Hydrothermal Synthesis of Nickel Manganese Oxide Nanowires as electrode material for super-capacitors



Name: Faiza Khalid

Reg. No: NUST2017NSE05-00000203146

This thesis is submitted as partial fulfilment of the

Requirements for the degree of

MS in Nanoscience and Engineerings

Supervisor Name: Dr. Mohsin Saleem

School of Chemical and Materials Engineering (SCME)

National University of Sciences and Technology (NUST)

H-12 Islamabad, Pakistan 2020

December,2020

Dedications

This study is sincerely dedicated to my beloved Baba, and my mother who have been my source of inspiration and gave me strength when I thought of giving up, who continually provide their moral, spiritual, emotional, and financial support.

Acknowledgments

All admiration to Allah Almighty. He is the One who bestows and gives the power to us to think, utilize our expertise in knowledge in achieving remarkable solutions for mankind in every field. Therefore, I express my greatest thanks to Almighty Allah, the universal and the architect of the world. Allah Almighty says in Quran: “ Read! In the name of your lord ” (Alaq; 1st revealed ayah). This Quranic verse sums up the entire importance of education in the lives of humans. I like to express my gratefulness to my very nice and respected supervisor Dr. Mohsin Saleem for their clear and patient guidance that directed me to fulfill my project and this thesis. Their cool and calm behavior motivated me to do my best. Their valuable suggestions and feedback contributed to this thesis. Also, I am very grateful to my Co-Supervisor, Dr. Aftab Akram, for their support, who helped and motivated me to do my research. I would also like to thank my parents, family members, and friends for their help, prayers, and their valuable suggestions

I want to thank Mr. Muhammad Usman, Mr. Muhammad Adnan, and Miss Tehmeena for their continuous support and motivation, which helped me at various stages during my master’s.

I also want to thank Miss Amna Ujala, Syed Aashir, and Mr. Saqib for their support, and they helped a lot during characterization and lab work. I acknowledge the support provided by the Materials Engineering Department of SCME for providing me a platform to perform my experiments and using my skills in research work.

My biggest appreciation to Saqlein (NG staff member) helped me in all the possible manners.

I acknowledge the financial aid and technical assistance provided by our department, SCME, during my research experience and made this project work memorable forever. Last but not least, I want to thank my family for their prayers, support, and confidence in me, without which I would not have been able to reach my full potential.

~Miss Faiza Khalid

Abstract

Nickel Manganese oxide Nanowires has been established as a promising electrode material. Nickel-Manganese oxide (NMO) nanowires were synthesized using a facile hydrothermal approach followed by annealing treatment. For a comparative study, Manganese oxide (NMO), Nickel manganese oxide, and activated carbon composite were also synthesized by the same method to examine the effect of doping for comparative study. The composition, structure and morphology of the samples were characterized by X-ray diffraction (XRD), scanning electron microscopy (SEM). The electrochemical performance of the material were examined by cyclic voltammetry (CV), and galvanostatic charge-discharge (GCD). NMO nanowires exhibit specific capacitance of 1634.4 Fg^{-1} at 1 Ag^{-1} , and After 10000 cycles, the specific capacitance of Ni-MnO_2 was still maintained at 96.5%, which shows excellent cycling stability. The results show that doping had a great influence on the electrochemical properties of the materials. Doping of nickel cation enhances the electrochemical performance of electrode material. NMO is a promising candidate for future energy storage devices.

Table of Contents

Chapter No 1	1
1.1 Introduction	1
1.2 Types of the energy storage system	2
1.3 Renewable energy resources	2
1.4 Energy Storage Devices	2
1.4.1 Batteries	3
1.4.2 Fuel cell.....	3
1.4.3 Capacitors	4
1.4.4 Supercapacitors	4
1.4.5 Types of Supercapacitors	5
1.5 Electrolytes in supercapacitors.....	10
1.5.1 Aqueous electrolytes.....	10
1.5.2 Organic electrolytes	10
1.5.3 Ionic liquids	11
1.6 Applications of supercapacitors	11
2 Chapter No 2.....	12
2.1 Electrode materials for supercapacitor.....	12
2.2 Carbon-based material for EDLC	12
2.3 Activated Carbon.....	12
2.4 Carbon Nanotubes	12
2.5 Graphene	13
2.6 Conducting Polymers	13
2.6.1 Polyaniline (PANI)	13
2.6.2 Polypyrrole (PPy).....	14
2.7 Metal Oxide.....	14
Chapter No 3	15
3 Literature review.....	15
3.1 Manganese Oxide.....	15
4 Chapter No 4.....	18
Experimentation and methodology	18
4.1 Aims and objectives	18

4.2	Synthesis method.....	18
4.2.1	Top to bottom approaches.....	18
4.2.2	Bottom-up approaches	18
4.2.3	Top to Bottom Approaches	21
4.2.4	Bottom-up approaches	23
4.2.4.2	Chemical vapour deposition	24
4.2.4.2.1	Advantages	24
4.3	Synthesis of Metal oxides	24
4.4	Materials required	24
4.5	Synthesis of Manganese Oxide (MO).....	25
4.6	Synthesis of Nickel Manganese oxide (NMO)	25
5	Chapter No 5.....	27
5.1	X-ray diffraction (XRD).....	27
5.1.1	Instrumental principle	27
5.1.2	Working	28
5.1.3	Crystal size measurement	28
5.2	SEM Analysis.....	29
5.3	Brunauer Emmett Teller (BET).....	30
5.4	FTIR Analysis	31
5.4.1	Instrumentation	31
5.5	Electrochemical Workstation	31
5.5.1	Supercapacitor performance testing.....	32
5.5.2	Electrode preparation	33
5.6	Cyclic Voltammetry	33
5.7	Galvanostatic Charge Discharge	34
5.8	Cyclic Stability.....	34
6	Results and discussions	35
6.1	Xrd analysis.....	35
6.2	FTIR Analysis	36
6.3	SEM Analysis.....	37
6.4	Electrochemical properties analysis	38
6.4.1	Cyclic voltammetry of MO.....	38
6.4.2	Galvanostatic Charge discharge.....	40
6.5	Energy Density and Power Density	41
6.6	Cyclic Stability.....	42

6.7	Raman Spectroscopy	44
7	References	47

List of Figures

Figure 1.1 Basic schematic of fuel cell	3
Figure 1.1.2 Schematic of conventional capacitors	4
Figure 1.1.3 comparison of the capacitor, supercapacitor, and battery	5
Figure 1.1.4 comparison of edlc, pseudo, and hybrid capacitors.....	6
Figure 1.1.5 charge storage mechanism in edlc [4]	7
Figure 1.1.6 types of super capacitors	8
Figure 1.1.7 storage mechanism of pseudo capacitors	9
Figure 1.1.8 hybrid super capacitor mechanism	10
Figure 3.1(a)number of research papers published on supercapacitors from 2000 to 2018. (b) publication on electrode material. (5)	15
Figure 4.1 schematic of sol gel method	19
Figure 4.2 schematic of a hydrothermal method	20
Figure 4.3 mechanical exfoliation of 2d materials.....	22
Figure 4.4 schematic of preparation of nickel manganese oxide nanowires	26
Figure 5.1 (a)xrd present at scme nust (b) schematic of xrd.....	28
Figure 5.2 (a)jeol-jsm- 6490la sem present at nust scme (b) schematic of sem	29
Figure 5.3 gemini® vii 2390 micro porosity analyzer.....	30
Figure 5.4 working of ftir.....	31
Figure 5.5 biologic vsp electrochemical workstation	32
Figure 5.6 electrode modification	33
Figure 6.1 xrd of nickel manganese oxide with activated carbon nanocomposites.....	36
Figure 6.3 ftir spectra of nickel manganese oxide	37
Figure 6.4 sem analysis of mo/nmo/nmoac	38
Figure 6.5 (a)cv of the mo (b) cv of nmo materials (c)cv of nmoac.....	40
Figure 6.6 (a)charge and discharge curves of sample mo at different current densities, (b) charge and discharge curves of sample nmo at different current densities.....	41
Figure 6.7 (a) charge and discharge curves at different densities.....	42
Figure 6.8 long-term cycling stability of sample mo and nmo	43
Figure 6.9 (a)specific capacitance of mo, nmo, nmoac different current densities(b) comparison of capacitance	44
Figure 6.10 raman spectra of manganese oxide and ni-doped manganese oxide	45

ABBREVIATIONS

MO_____Nickel Oxide

NMO_____Nickel Manganese Oxide

NMOAC_____Nickel Manganese oxide

activated carbon nanowires

CV_____Cyclic Voltammetry

GCD_____Galvanostatic charge-discharge

Chapter No 1

Introduction to energy storage devices

1.1 Introduction

Energy has become the main focus in the scientific and industrial communities due to the fast development of the global economy and climate changes. There is an as urgent need for an efficient, clean, and renewable energy source and energy storage technique because the world is facing an energy crisis daily.

The world is facing a severe energy crisis. The need of the hour is to shift towards sustainable and green energy products[1]. There has been a lot of research carried out on Li-ION batteries and fuel cells to make them efficient but the poor power proficiency and high relative maintenance cost hinders them to make in practical aspects. In the recent times, a great great attention has been paid to supercapacitors , it is due to their high charge-discharge rate, long life cycle, exceptional power density, Supercapacitors, also known as ultra-capacitors or electrochemical capacitors. The demand for energy storage devices is increasing day by day due to the energy crisis in th world.

The need of the hour is to develop new sustainable, renewable electrode materials for the storage of electrical energy. Electrical energy is stored in two different ways. One is the “faradic process” in which redox reaction occurs due to electrochemically active material. Due to this redox reaction, the electrical current flows between two electrode systems at different potentials. This type of phenomenon is used in most batteries. The other way to store electrical energy is “non-faradic” or “electrostatically.” This phenomenon is used in the conventional capacitor, also called electrolytic capacitor.

On the other hand, the capacitor has almost unlimited cyclability as it is not accompanied by chemical and phase changes during the energy storage process. However, conventional capacitor with the advantage of high stability is limited with their low energy density ($\leq 10\text{-}2\text{W/Kg}$). However, these capacitors are combined with liquid electrolyte and high specific surface area electrode material like graphene, activated carbon materials. It can achieve a high capacitance up to several hundred Farad per gram (F/g)

in aqueous electrolyte [2]. This combination produces another storage device called a supercapacitor or ultra-capacitor, or electrochemical capacitor (EC). So, supercapacitor acts as a bridge between conventional capacitors and batteries.

Passive components are required in all electronic applications to store electrical energy in volume and weight as small as possible. The power needed by an application and the speed of the storage process determines the type of energy storage device to use.

1.2 Types of the energy storage system

- Batteries
- Fuel cells
- Capacitors
- Supercapacitors
- Symmetric devices
- Asymmetric devices

1.3 Renewable energy resources

Renewable energy resources are those who cut off our dependence on non-renewable energy resources. These resources do not deplete, and they can reuse again for our convenience. There are many forms of renewable energies which include:

- Hydrothermal energy
- Geothermal energy
- Solar energy
- Wind energy
- Biomass

Renewable energy sources should be use as they are natural and better. They are also cost-effective and ‘green.’ They do not create havoc for the environment. They are getting cheaper by the day as technology is progressing. New technologies are also being explored in them.

1.4 Energy Storage Devices

The need for energy storage devices increases with the increase of renewable energy resources[3]. Energy storage systems are divided into five major categories

- Mechanical system
- Chemical system
- Electrochemical system
- Electrical system

- Thermal system

The most common energy storage devices that come in electrochemical and electrical systems are batteries and supercapacitors.

1.4.1 Batteries

Batteries are the most efficient source of energy storage systems. They have high energy density and a limited life cycle in secondary batteries where energy is stored reversibly – since energy is stored through faradic reaction. These conversions are usually associated with phase changes. The charge-discharge process in secondary batteries is usually accompanied by volume changes and irreversibility of electrochemical reaction leading to the limited life cycle of secondary batteries.

1.4.1.1 Types of batteries

- Primary Batteries
- Secondary Batteries
 - Lead-acid batteries
 - Li-ion batteries
 - Sodium-ion
 - Li-polymer

1.4.2 Fuel cell

A fuel cell is also used as a device that converts chemical potential energy (energy stored in molecular bonds) into electrical energy. For example, a PEM (Proton Exchange Membrane) cell uses hydrogen gas (H_2) and oxygen gas (O_2) as fuel. The products of the reaction in the cell are water, electricity, and heat.

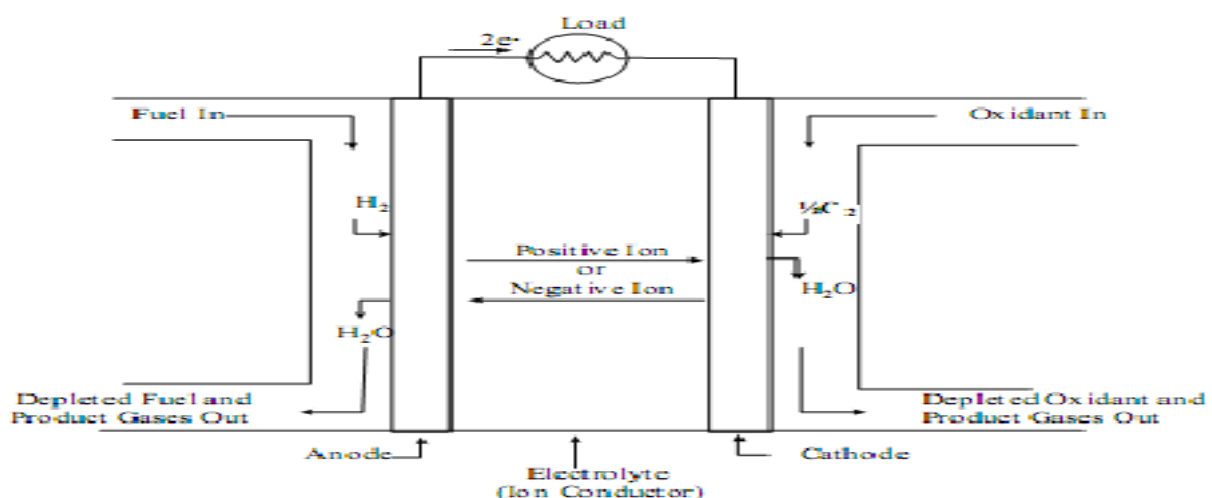


Figure 0.1 Basic schematic of fuel cell

1.4.3 Capacitors

Capacitors are the most efficient devices to store energy. It contains two or three-electrode systems separated by an electrolyte. The charge is stored b/w electric field. They have low energy density. Capacitors store energy, which can be measure as capacitance (C) is measured in Farad (F) and can be calculated by

$$C = A \times \epsilon \times d \quad 1$$

Here

A = Surface area

ϵ = Dielectric constant

d= Separation distance.

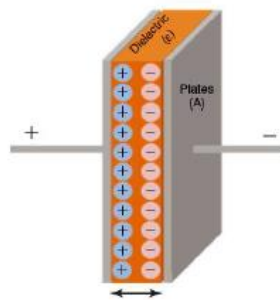


Figure 1.0.2 Schematic of Conventional capacitors

Conventional capacitors can accumulate energy between pico and microfarads

1.4.4 Supercapacitors

Supercapacitors are the potential candidate for next-generation energy storage devices. They are also called electrochemical capacitors, or ultra-capacitors. Their ability to provide higher energy density and high power capacity as compared to batteries have attracted their interest worldwide. Because of these advantages, supercapacitors can be widely use in hybrid vehicles, electronic devices, and digital products.

Research being carried out now are on how to improve the energy density, to be use in a broader range of applications. The few factors which play the cardinal role in the performance of supercapacitor are electrochemical properties of electrode materials used, the type an dcomposition of electrolyte and range of opertaional voltage.while all these factors are primarily

responsible for Performance; new researches are mostly focused for better performance are carried out on the development of new electrode materials. These devices have been exploited for their potential to store more energy and for long cyclic life. The specific capacitance is defined as:

$$Q = C \times V \dots\dots\dots (2)$$

Where,

C= specific capacitance, V= Operating window, and Q= Charge stored

The supercapacitor is known as a promising candidate since it shows energy-storing. Supercapacitors worked by storing charges via redox reactions. These capacitors include carbon, transition metal hydroxides/ oxides and conducting polymers in them as a electrode material. Capacitance is achieved by faradic charge transfer mechanism. This Charge transfer means transfer of charge across the electrode from one to another or by intercalation due to high power output and low cost.

Characteristics	Capacitor	Supercapacitor	Battery
Specific energy (W h kg ⁻¹)	< 0.1	1–10	10–100
Specific power (W kg ⁻¹)	≥10,000	500–10,000	< 1000
Discharge time	10 ⁻⁶ to 10 ⁻³	s to min	0.3–3 h
Charge time	10 ⁻⁶ to 10 ⁻³	s to min	1–5 h
Coulombic efficiency (%)	About 100	85–98	70–85
Cycle-life	Almost infinite	> 500,000	about 1000

Figure 1.0.3 Comparison of the capacitor, supercapacitor, and Battery

1.4.5 Types of Supercapacitors

Supercapacitors have 3 types, Given below

- Electrical double layer supercapacitor
- Pseudo capacitors
- Hybrid Capacitors

Electric double layer capacitors	<ul style="list-style-type: none"> ▪ Carbon aerogels ▪ Activated carbons ▪ Carbon fibers ▪ Carbon nanotubes
Pseudo-capacitors	<ul style="list-style-type: none"> ▪ Metal oxides ▪ Conducting polymers
Hybrid capacitors <ul style="list-style-type: none"> □ Asymmetric □ Composite □ Battery-type 	<ul style="list-style-type: none"> ▪ Carbon materials, conducting polymers ▪ Carbon materials, metal oxides

Figure 1.0.4 Comparison of Electric Double Layer, Pseudo, and Hybrid Capacitors

1.4.5.1 Electrical double layer Supercapacitor (EDLCs)

In this type of capacitor, the charge storage occurs electrostatically between the Helmholtz layer. Mostly carbon-based electrode materials (like Carbon nanotube, activated carbon, carbon aerogels) are used in these types of capacitors. An electrolytic capacitor also contains electrolyte whose capacitance also depends upon metal. As there are no electron transfer reactions involved; therefore, they have no limitation due to electrochemical kinetics (Pseudo capacitor involved electron transfer, so they have such limitations). Therefore, EDLC has higher energy and power densities than Pseudo capacitors.

1.4.5.2 Mechanism of electrical double layer capacitor

However, EDLC is mostly confused with the electrolytic capacitor (as it also stores charges electrostatically). The conventional capacitor is a dielectric one such as a film capacitor and ceramic capacitor. These consist of two electrodes, which are separated by the dielectric material, which electrostatically stores the charges. On the other hand, EDLC stores the charges by Helmholtz electrical double layer that appears on the surface when electrode material is exposed to electrolyte which contain free ions that move under the influence of electric charges. It is thus known as diffuse layer. As electrolytic capacitor also contains electrolyte, but its capacitance depends entirely on the oxide films that are present on metal plates by performing anodic electrolysis; to become dielectric ones. As EDLC has a large surface area than a dielectric capacitor and having more smaller separation distance from the molecule

separator, such as a water molecule of an order of 0.3-0.8nm. This is smaller than the insulating oxide layer of an order of 10-100nm in the conventional electrode and thus giving high specific capacitance to EDLC by a factor of 10,000, so there is only adsorption-desorption of ions at this large surface area of the electrode.

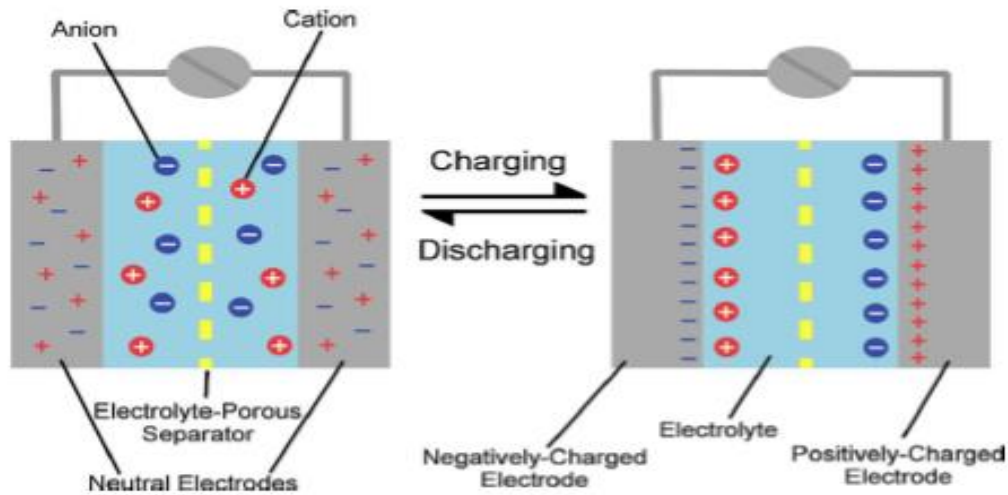


Figure 1.0.5 Charge storage mechanism in EDLC [4]

EDLC has a long cycle of life because of physical charge transfer occurs. EDLC capacitance can be express as

$$C = \frac{A\epsilon}{4\pi D}$$

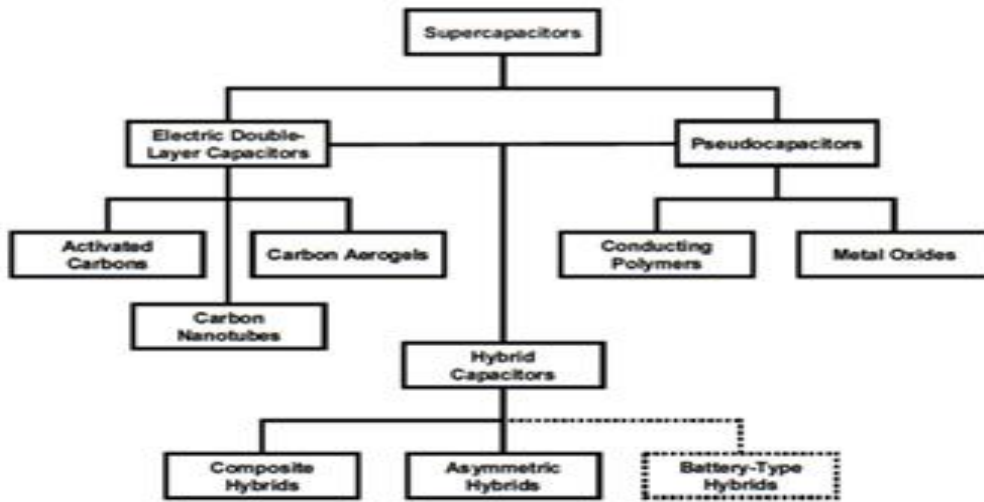
Where

A= Surface area of the electrodes

ϵ = dielectric constant

d= effective thickness of the double layer

TYPES OF SUPERCAPACITORS



* Marin S. Halper and James C. Ellenbogen, "Supercapacitors: A Brief Overview", March 2006, MITRE Nanosystems Gro

Figure 1.0.6 Types of Super Capacitors

1.4.5.3 Pseudo capacitors

A pseudo capacitor is different from the EDLCs as they involved a highly fast and reversible faradic reaction between electrolyte and electrode material. Different metal oxides (MnO^{2-} , Ru^{2-} etc.) and conducting polymers (polyaniline, polypyrrole, etc.) show pseudocapacitance behavior[5-7]

Pseudo capacitors work like rechargeable batteries, which involve a faradic process, and therefore, there is confusion between these two types of charge storing devices. The charge storage mechanism of pseudo capacitor and Battery is quite different. The pseudo capacitor involves a highly fast and reversible faradic (redox) reaction on the surface or close to the surface of an electrode material having a distance of

$l \ll (2Dt)^{1/2}$ (Here D (cm^2s^{-1}) is the diffusion coefficient for the ions and t (s) is the time while l is the diffusion thickness. So pseudocapacitors faradic reaction is not affected by the diffusion limit and phase transformation of the electrode material. Simply we can say pseudocapacitance is due to the spread of the charge while battery capacitance is due to the transfer of electrons between electrodes. The pseudocapacitance is produced from three mechanisms (i) underpotential deposition, (ii) surface controlled electrochemical rapid reactions, and (iii) fast ion intercalation. The energy is store in the form of crystal lattice through electrochemical

responses affected by the phase transformation in batteries. The diffusion of reactant molecules/ions, and chemical binding changes, thus resulting in more kinetic stagnant, low reversibility, and the electrochemical process has diffusion-controlled kinetics. That is why batteries have low capacitance, power density, and short life.

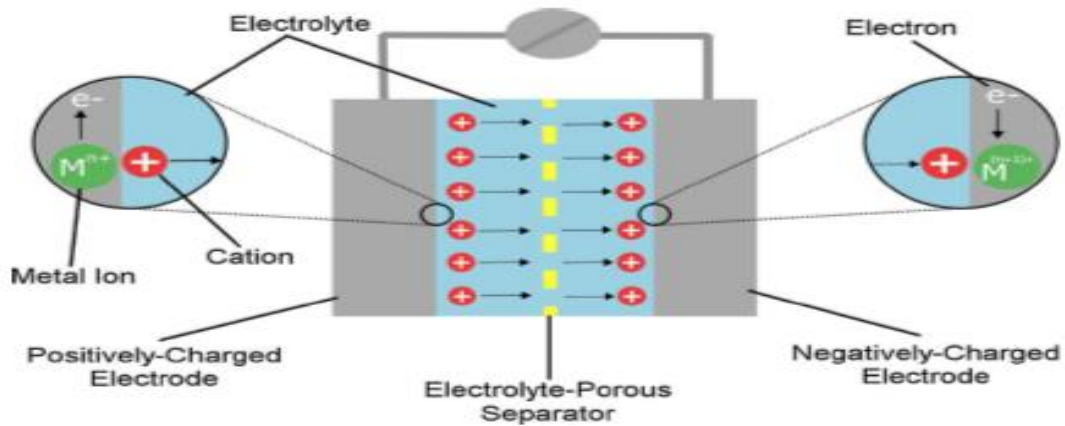


Figure 1.0.7 Storage mechanism of Pseudo Capacitors

1.4.5.4 Hybrid Capacitors

They are also called battery type or asymmetric supercapacitors. They are formed by combining both EDLCs and pseudo capacitor materials, i.e., incorporating metal oxide into graphene or other carbon-based materials or incorporating conductive polymers into carbon-based materials. So, one kind of material stores charge faradaic ally and other stores charge electrostatically. The key characteristics of hybrid supercapacitors are

- Excellent specific capacitance
- Power Density
- High Energy Density
- Good cyclic stability

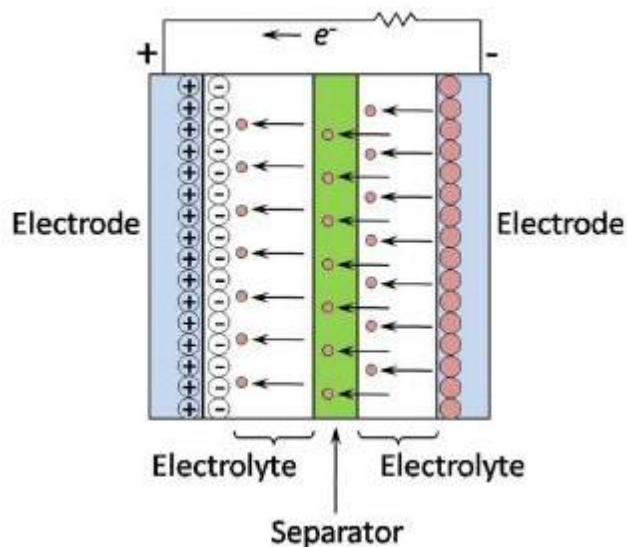


Figure 1.0.8 Hybrid Super Capacitor Mechanism

1.5 Electrolytes in supercapacitors

Electrolytes are another main parameter that affects the performance of supercapacitors. The ion concentration is more important for the flow of charge. If electrolyte concentration is below 0.2 M than the performance of the device is reduced. This electrolyte should have high electrochemical stability, low resistivity, wide potential range, low volatility, high ionic concentration, cost-effective, low toxicity, and available in high purity. The electrolytes are of three types

- (i) Aqueous electrolytes
- (ii) Organic electrolytes
- (iii) Ionic liquids

1.5.1 Aqueous electrolytes

Aqueous electrolytes like H_2SO_4 , Na_2SO_4 , KOH give low resistance and high ionic concentration than organic electrolytes. Aqueous electrolytes can be easily prepared in pure form. However, there is one disadvantage with aqueous electrolytes that their potential window is very small, which is about 1.2V, much smaller than organic electrolytes.

1.5.2 Organic electrolytes

organic electrolytes have a vast potential window as high as 3.5V, making them promising candidates for supercapacitors. Commonly used organic electrolytes are propylene carbonate

and acetonitrile. The main issue with organic electrolyte is the water content that needs to be below 3-5 ppm.

1.5.3 Ionic liquids

The melted or it is liquefied salt; then it is called ionic liquid. The properties of ionic liquids are; wide potential range up to 6V, typically about 4.5V, high chemical and thermal stability. Commonly studied ionic liquids are imidazolium and pyrrolidinium

1.6 Applications of supercapacitors

The best use of supercapacitors is their role in applications with high reliability and short load cycles, such as energy recapture sources such as forklifts, load cranes and electric vehicles, power quality improvement. The most in demand applications of supercapacitors are Fuel cell vehicles and economical and Environment friendly Electric vehicle. Merger of Supercap with batteries or fuel cells serves as a short time energy storage devices. Depolymerizing rapid power capability for energy storage. The supercapacitor have High energy density as comparison to conventional capacitors but have less energy density than that of batteries or fuel cells.

Chapter No 2

Electrode Materials for Supercapacitors

2.1 Electrode materials for supercapacitor

In recent years, major progress has been made on supercapacitor materials. They have some disadvantages, which include high production cost and low energy density. To overcome the low energy density, research is going on the development of new electrode materials for supercapacitors.

Nanostructured materials are focused on high-performance supercapacitors. The capacitance is strongly reliant on the surface area as it has a direct influence on capacitance performance. The capacitance of a material is high; it exhibits large porosity and pore volume for a given surface area. Electrode materials are classified into three major types.

2.2 Carbon-based material for EDLC

As stated, earlier carbon-based materials are suitable for electrical double-layer capacitors because of their properties i-e low cost, high conductivity, environment friendly, good chemical stability, high specific surface area. The cyclic voltammogram of carbon-based material is rectangular without any redox peaks showing that stores charge in the form of Helmholtz electrical double layer. The galvanostatic charge-discharge curves of carbon-based materials are symmetrical, indicating a high Columbia utility ratio of the electrostatic charge storage method. These materials are most widely used for the supercapacitor due to the ease of processing, and abundance is quite high and cost-effective. Most common electrode materials are classified as

2.3 Activated Carbon

It is mostly use for supercapacitors. A significant advantage of activated carbon is the high surface area and less expensive compared to carbon nanotubes and graphene. Its precursors are obtained from natural resources. Activation of precursors can be achieved by the carbonization process, which is the heat treatment process under an inert atmosphere.

2.4 Carbon Nanotubes

CNTs are also a versatile material for the supercapacitor applications are synthesized by the decomposition of hydrocarbons. Depending upon the process, SWCNTs or MWCNTs can be synthesize. CNTs exhibit high conductivity, and the surface area also mechanical as well as

chemical properties are excellent. Supercapacitors which made from CNTS utilize its surface area up to maximum extent results the electrode developed by CNTs exhibits almost the same capacitance as an activated carbon electrode

2.5 Graphene

Graphene is a one-atom-thick, two-dimensional, hexagonal sp² hybrid, honeycomb allotrope of carbon just like graphite, fullerenes, and CNTs. Graphene possesses remarkable properties like thermal stability, high mechanical strength (~1TPa), and high conductance. These graphene exhibits a high theoretical specific surface area (2675 m²/g), making it a good candidate for the electrical double layer.

2.6 Conducting Polymers

The conducting polymer possesses pseudocapacitance behavior due to redox reactions. Oxidation occurs when ions are transferred to polymer, whereas reduction occurs when polymer releases those ions into an electrolyte. These are several advantages of using conduction polymer as an electrode material for supercapacitor materials are

- Low cost
- Environment-friendly
- high conductivity
- high working window
- High Capacitance
- Low Equivalent resistivity and conductivity
- Large Surface Area

Common CP used for electrode materials are following

2.6.1 Polyaniline (PANI)

PANI is a conducting polymer. Besides carbon-based materials, it plays an essential role in supercapacitors due to low cost, high specific capacitance, and flexibility as well as ease of processing. The biggest drawback which limits PANI applications is its stability and degradation at a high potential. Therefore, the combination of PANI with other materials enhance its stability. PANI is synthesized by polymerization of aniline monomer with an oxidant used is ammonium persulfate, or iron chloride[8]-[9]-[10]-[11] PANI has different oxidation states

- Emeraldine base (EB)

- Leucoemeraldine (LE)
- Per nigraniline (PE)

PANI-EB is possessed high conductivity and stability as compared to the other two states. When PANI is used in the supercapacitor, the charge storage mechanism is a redox reaction. It is used in batteries, supercapacitors, and fuel cells.

2.6.2 Polypyrrole (PPy)

It is also a conducting polymer, used in batteries, sensors, fuel cells, and supercapacitors. The advantage of PPy is the ease of synthesis, good redox activity, low density, and high conductivity. It can store a greater amount of charge as compared to EDLC. It can synthesize by the chemical polymerization by using the oxidation agent. The concentration of dopant affects the Stability and capacitance performance of PPy [12-14].

2.7 Metal Oxide

Metal oxides exhibit high specific capacitance as well as stability, which makes them one of the best candidates of electrode material as energy storage devices. Researchers are focused on metal oxides because of high energy density and superior electrochemical performance as compared to other materials. There are three requirements that which metal oxide meet those requirements can be considered for electrochemical supercapacitors application

- Metal oxide needs to be conductive
- Two or three oxidation states exist or coexist
- During reduction, protons can intercalate into the lattice of oxide

Ruthenium oxide (RuO_2), Vanadium oxide (V_2O_5), Nickel oxide (NiO), Cobalt oxide (Co_2O_3), Iron oxide (Fe_2O_3) and Manganese oxide (MnO_2) are common oxide material which meets the basic requirement and employs as supercapacitors because of superior properties[15]-[16]-[17]-[18].

Chapter No 3

Literature review

Supercapacitors, in recent years, have drawn more attention from the researchers. Less energy density is the main problem for supercapacitor. Advancement in the electrode material and technology; they are filling the gap between the fuel cell and batteries. The figure shows the material focused on recent years as well as the number of research work conducted on supercapacitors in the last two decades.

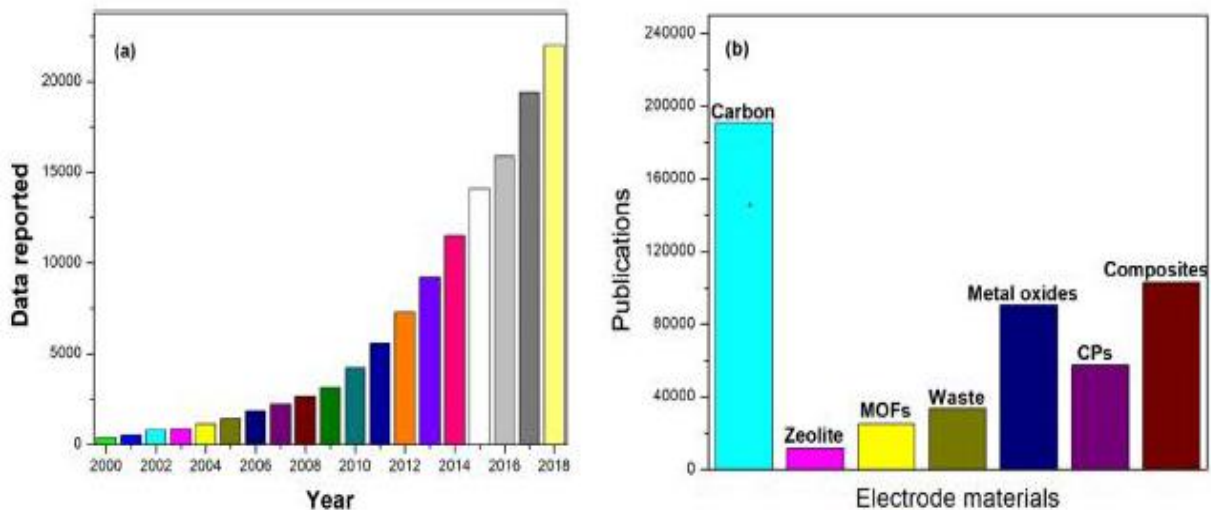


Figure 3.1(a) Number of research papers published on supercapacitors from 2000 to 2018. (b) Publication on electrode material. (5)

3.1 Manganese Oxide

Manganese oxide is considered as an active member of electrode materials. Due to its variable valency it forms different oxides which are acidic, basic, and amphoteric in nature. For example, the oxides MnO_2 and Mn_2O_3 are basic because, in these oxides, the oxidation state of manganese is +2 AND +3. In the case of Mn_2O_7 , which is strongly acidic because of a high oxidation state. But the capacitance of the MnO_2 electrode is vitally affected and dominant because of reversible redox reaction in which cations and protons are exchanged with electrolyte.

1. Jie dong *et al.* explained the preparation of nickel manganese oxide by sol-gel for electrode material for supercapacitors. The capacitance of Ni-MnO₂ was found about 252.61 F/g. it retained its capacitance for 2000 charge/discharge cycles, maintaining the specific capacitance at 74.36%, which was verified the prominent cycling stability.
2. Qianqian Li *et al.* reported that the synthesis by co-precipitation. The investigation of electrochemical performance using 6 molar KOH proves that NMO exhibits specific capacitance (Cs) 130F/g at 1A/g.
3. Jiayu Hao *et al.* reported that the nanoneedles of nickel doped manganese oxide were synthesized by the hydrothermal method by changing the concentration of nickel ions using 0.1 molar KOH electrolyte. The electrochemical performance shown by 2.22% doping of nickel ions shows higher current density and faster reaction kinetics.
4. Chen *et al.* reported that the CdS anchored in three-dimensional graphite cage showing specific capacitance of 511 F/g at 5A/g and retains its 90.1% capacitance after 5000 cycles at 10A/g.
5. Idrees Khan *et al.* reported that the MnO₂ nps/AC carbon composites prepared by chemical reduction method. MnO₂ nps were found of cylindrical and spherical shape by morphological analysis. These analysis also corroborated the dispersion of MnO₂ nps. FTIR is used to investigate the formation of particles. Zetasizer's study represented that the Mn NPs had the uniformity of particle size around 100 nm and had zeta potential of - 20 mV, demonstrating its stability for suspension.
6. Young Chen *et al.* reported that the asymmetric electrode material of MnO₂ and MWCNT's nanotubes prepared in three simple steps. The 1 mol L sodium sulfate is used as an electrolyte to check the electrochemical performance of the electrode material. The specific capacitance was obtained by this composite (806 F/g at the current density of 1 A g).
7. Ao Xiao *et al.* reported that the synthesis protocol porous δ-MnO₂ nanosheets. The effect of temperature on morphology of MO using XRD, SEM also investigated. They have reported the effect of hydrothermal temperature on the morphology of samples. It has been stated that material prepared at 150 C have high specific capacitance and higher cyclic stability.

8. Yu Li *et al.* reported that the formation of the snowflake (3D) like the structure of manganese oxide prepared by hydrothermal method. These 3D-MnO₂ are efficient and have less defects than that of single-phase MnO₂ as electrode materials. There are various characterization techniques XRD, BET, XPS are used for the investigation of synthesized materials. It has possessed the highest specific capacitance (C_m) (260.5 F/g at a current density of 0.3 A/gs, and showing good performance and excellent cycling stability (94.7% capacitance retention after 3000 cycles).

9. Xianlin bai *et al.* reported that the manganese dioxide (MnO₂) cauliflower-like morphology studied with a change in dwell time in this paper. It has been observed that hydrothermal dwell time have effected the morphologies of MnO₂. The specific capacitance for needle-like α-MnO₂ Nanorods was higher as they have high specific surface while the specific capacitance for cauliflower-like δ-MnO₂ particles was found to be less than the others. The specific capacitance shown by the MnO₂ is 311.52 F/g at 0.3 A/g. These results proved the manganese oxide as a potential candidate for energy storage systems.

10. Wei Gao *et al.* reported that the MnO₂ synthesized via a simple method to investigate its electrochemical performance. MnO₂ has been studied as it possesses high theoretical capacitance value and operated in large potential window. However, the difference between practical and theoretical capacitance limits it uses for future applications. To improve the capacitive properties of MnO₂ as electrode materials with interesting capacitive performance. The morphological analysis were carried out with different characterization techniques.

Chapter No 4

Experimentation and methodology

4.1 Aims and objectives

This project aims to prepare MO /NMO/AC composite to investigate its charge storage application. The sequential targets were;

- (i) The synthesis of Manganese Oxide nanowires, Nickel doped manganese oxide nanowires and AC composite using hydrothermal approach.
- (ii) Structural Characterization of the synthesized composite by XRD, SEM, and FTIR.
- (iii) Electrochemical performance testing of prepared materials using the electrochemical work station.
- (iv) Interpretation of the results for the use of synthesized material as an electrode in supercapacitor devices.

4.2 Synthesis method

For the synthesis of manganese-nickel oxide nanowires, top to down approaches was used. Most of the oxides were synthesized by bottom-up approaches and discussed in detail below.

4.2.1 Top to bottom approaches

- Lithographic techniques
- Etching
- Ball Milling
- Sputtering

4.2.2 Bottom-up approaches

- Co-precipitation
- Sol-gel method
- Chemical reduction method
- Hydrothermal synthesis (adopted)
- Microemulsion method

4.2.2.1 Sol-gel method

In this method, firstly, the precursors were mixed to form a solution process is called hydrolysis, then transform into gel called dehydration, followed by drying through thermal treatment; in this phase, the liquid removed from the gel.

4.2.2.1.1 Advantages

It is a simple and cost-effective method

- High purity
- Excellent homogeneity
- Low-temperature technique

4.2.2.1.2 Limitations

- Weak bonding
- Porosity control is difficult

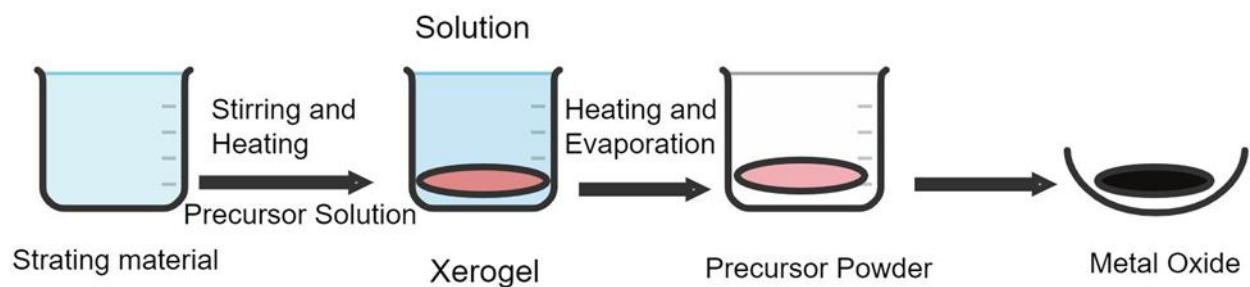


Figure 0.1 Schematic of sol gel method

4.2.2.2 Hydrothermal Process

Hydrothermal/Solvo thermal is the process in which chemical reaction occurs in temperature and pressure. The hydrothermal reactor or sealed vessel is used for this process, and precursors were dispersed in the solvent and placed at a temperature above its boiling point; autogenous pressure is developed by heating. In the case of water, it called hydrothermally and incased of any other solvent it is called solvo thermal process.

4.2.2.2.1 Advantages

- Simple method
- Morphology control is easy and precise by changing time, temperature and concentration, and solvent type.

4.2.2.2.2 Limitations

- Expensive autoclaves and reactors
- Safety issues

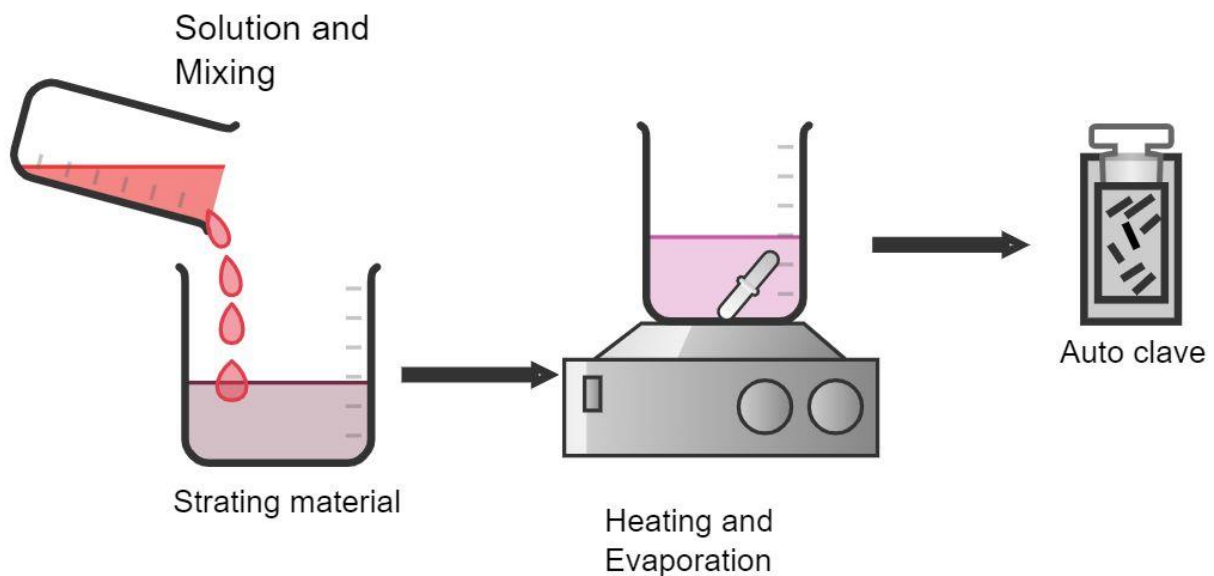


Figure 0.2 Schematic of a hydrothermal method

4.2.2.3 Chemical Co-precipitation

Coprecipitation is used for the synthesis of nanoparticles. In this process, the residues taken out of the solution. Precipitation involves contaminants into precipitates. In this method, the precursor was dissolved in the presence of a precipitation agent to form a homogeneous solution followed by centrifugation drying, milling, and calcination process at elevated temperature.

4.2.2.3.1 Advantages

- Low cost
- Environment-friendly
- Large scale synthesis

4.2.2.3.2 Limitations

- Poor crystallinity
- Agglomeration
- Size distribution and control is exceedingly difficult

4.2.2.4 Microemulsion

A microemulsion is another synthesis technique of oxide nanoparticle in which two phases are mixed, and chemical reactions occur. The aqueous phase is metal salts and surfactants, while another phase maybe oil and water. Two types of microemulsion were used direct and reversed oil dispersed in water and other water dispersed in oil, respectively.

4.2.2.4.1 Advantages

- Uniform properties can achieve
- Good Pore size distribution

4.2.2.4.2 Limitations

- Surfactant removal is not easy

4.2.3 Top to Bottom Approaches

2D materials exfoliation [6] is one high area of interest to prepare mono or a few layered materials. Exfoliated materials carry importance both in their potential applications and fundamental studies. Materials obtained from exfoliation of graphite and TMDs carry importance as they provide a break-through in flexible electronics and optoelectronics devices. In 2D materials, strong in-plane bonding[16],[19], and weak bonding between their layers, these layers can be separated from each other to increase surface area and potential properties of materials. Exfoliation can be done by

- Mechanical exfoliation
- Liquid phase exfoliation

4.2.3.1 Mechanical exfoliation

In this method, the layers are separated by applying some mechanical forces.[20] In this method, high-quality mono sheets can also form. Graphene was synthesized using bulk graphite by “scotch tape method” [21] This method is popular as it produces intrinsic sheets, and a large area of research is focused on it now.

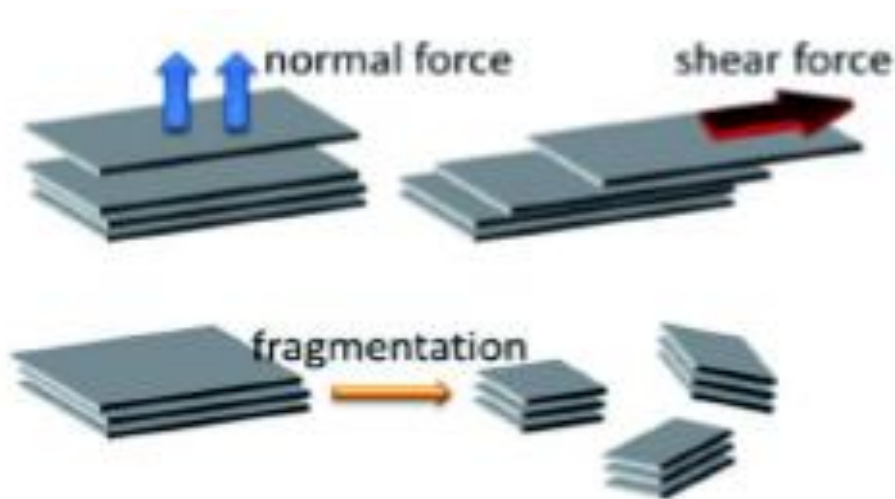


Figure 0.3 Mechanical Exfoliation of 2D materials

4.2.3.1.1 Advantages

- Generally, by this method, pristine quality sheets are obtained.

4.2.3.1.2 Limitations

- Low yield is obtained in this process.
- Also, in this method, there is a lack of scalability [22].
- Not applicable for large scale production.
- Sheet size and thickness controlling is an issue.

4.2.3.2 Liquid phase exfoliation

In this method, solvents are used to intercalate the layers of the compound. Those solvents are used whose surface energy matches with that of the crystal lattice of the layered material.

Sonication produces nanosheets that are stabilized in a suitable solvent in the reaction mixture or dispersion[23]. Some surfactants may also be added in them to obtain well-defined structures. Sonication-assisted exfoliation is now used extensively for the preparation of mono-, few-layered structures from bulk. In sonication, sound energy applied, which results in shear forces. Cavitation bubbles are produced when collapse, peel off the layers.

The solvent is a critical choice; i.e., it must facilitate the delimitation process. It should sustain highly stabilized dispersions with a high concentration of 2D exfoliated sheets. Sometimes a combination of solvents may also be applied for efficient exfoliation of materials. Insolvents, N-methyl-2-pyrrolidone (NMP) is most common. NMP has a surface energy of $\sim 40 \text{ mJ m}^{-2}$, which matches the surface energy of many-layered materials[24]. In NMP, one can achieve stable dispersions of graphite with up to 40 mg ml^{-1} has surface energy $\sim 75 \text{ mJ m}^{-2}$.

4.2.3.2.1 Advantages

- A high yield is obtained in this process.
- This method is not air sensitive.
- No chemical reactions take place.
- The highly crystalline product is obtained.
- This method is so simple and cost-effective

4.2.3.2.2 Limitations

The solution-based exfoliation contains residual chemicals present in them, affecting the properties of Nanosheets like graphene. The solvent may be volatile and toxic too.

This method can cause defects in 2D structures and reduce flake size to a hundred nanometers.

4.2.4 Bottom-up approaches

Also, there are many ways to develop 2D materials via bottom-up approaches like

1. Wet chemical synthesis
2. Chemical vapour deposition

4.2.4.1 Wet chemical synthesis

By this technique, the target materials are prepared using precursors, and chemical reactions take place in the solution. One widely used wet-chemical method for nanomaterials includes

template synthesis, hydro/solvothermal synthesis, self-assembly of Nanocrystals, and soft colloidal synthesis.

4.2.4.1.1 Advantages

- All 2D materials, sheets and metals were successfully synthesized by this technique.
- A high yield of 2D nanomaterial at very low cost can achieve.
- Control on the morphology of nanomaterial is more in wet chemical methods.

4.2.4.1.2 Limitations

Hard to achieve a single layer of 2D Nanosheets

4.2.4.2 Chemical vapour deposition

CVD involves the chemical reaction of gaseous precursors at a surface of the substrate to achieve the deposition of the desired material. Control of the reaction kinetic is possible by controlling temperature, time, pressure, and yield concentration.

4.2.4.2.1 Advantages

- Heterogeneous reactions take place, which forms good quality films.
- In many systems, fast deposition takes place with good step coverage.

4.2.4.2.2 Limitations

- Elevated temperature is required to initiate reactions.
- Sometimes chemicals and particle contamination occur.

4.3 Synthesis of Metal oxides

The hydrothermal method is adopted for the synthesis of metals oxide Nanoparticles because of control in the morphology and structure i-e nanorods, nanoflowers, nanowires can be attained by varying temperature and time of the reaction.

4.4 Materials required

All the chemicals were purchased from Sigma Aldrich and used as received without any further purification or distillation process. All solutions for cyclic voltammetry were prepared in deionized water (DI). All the following chemicals are

- Manganese acetate
- Nickel acetate

- Ethanol
- Potassium Hydroxide
- Nafion
- Acetone
- DI water
- Activated Carbon

Apparatus used for the preparation of oxides was

- Teflon lined stainless steel autoclave
- Oven
- Magnetic stirrer
- Hotplate
- Beakers
- Petri dishes
- Weighing balance
- Fume hood
- Vacuum filtration
- Filter papers
- Muffle Furnace

4.5 Synthesis of Manganese Oxide (MO)

MO was synthesized via a simple hydrothermal method followed by calcination. First, 0.6 mmol manganese acetate, 1.8mmol of KMnO_4 were slowly mixing into deionized water. The prepared solution with continuous stirring for 30min. The homogeneous mixture was transferred into the 50 ml of Teflon lined stainless steel autoclave. The autoclave was kept in the oven at 130C for 5h. Then, the autoclave was naturally cooled to room temperature, and the solution was filtered several times using filtration assembly with DI water and ethanol, respectively. Finally, precipitates were filtered out by vacuum filtration. Afterwards, the sample was dried at 60 °C for 12h and then annealed at 350 °C at 2 °C /min in a muffle furnace for 2h to obtain the black precipitates of MO.

4.6 Synthesis of Nickel Manganese oxide (NMO)

All chemicals were purchased commercially and used as received without further purification. The pure nanowires of Nickel Manganese oxide (NMO) were prepared by facile hydrothermal synthesis using Manganese acetate(0.6mmol), Nickel acetate (0.6mmol), and KMnO_4

(1.8mmol of) were slowly added into deionized (DI) water (18ml). The prepared solution was magnetically stirred for 30 minutes. Then, the dispersed solution was transferred into a 50 mL Teflon-lined autoclave, sealed and heated at 140C for 12 h. Finally, the obtained precipitate dried in an oven at 60 °C for 12 h. then annealed at 450C for 2h. The nickel manganese oxide(NMO) composite with activated carbon was also prepared using nickel acetate. The composite of NMO and activated carbon(AC) synthesized by adding 25% AC to the mixture solution. The reaction protocols and the temperature is the same as above.

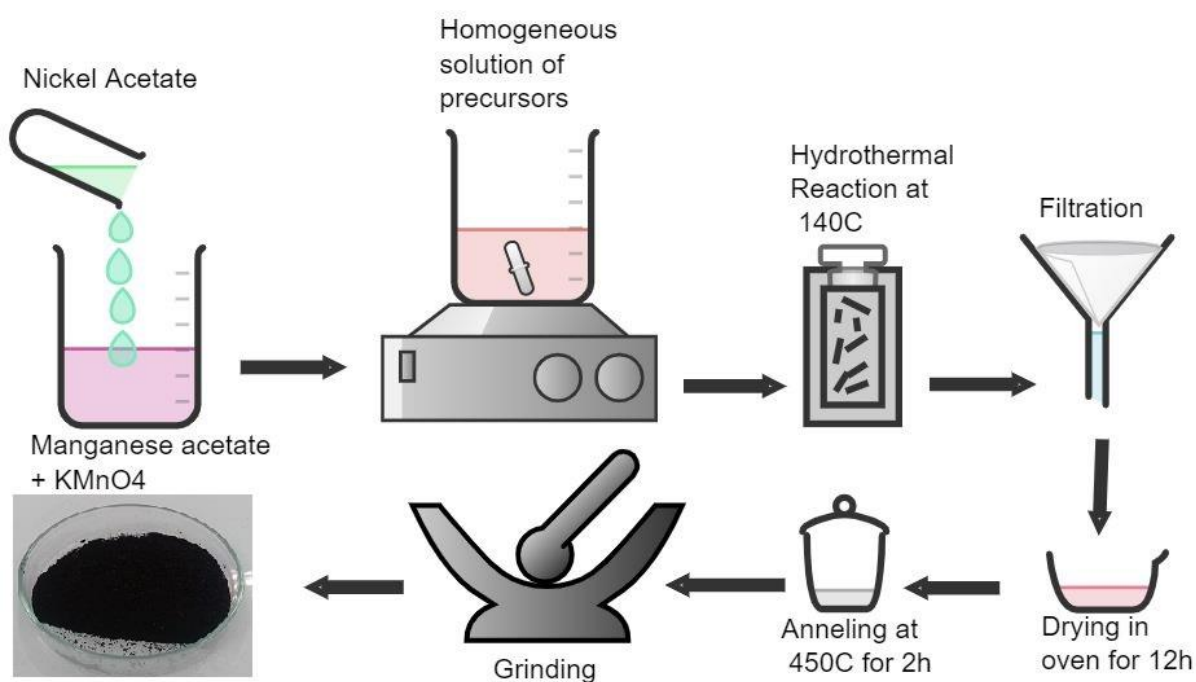


Figure 0.4 Schematic of preparation of nickel manganese oxide nanowires

Chapter No 5

Characterization techniques

Most characterization methods are used on the sample in powder forms or solutions forms. It is due to thermodynamics in which molecules are easily interpreted on the basis of their physical size and macro structure. The characterization techniques in material science uses the sample in powder and solution forms for the analysis of crystal structure and analysis of physical features such as grain boundaries and morphological analysis.

The following are the techniques used for the material characterization

- X-rays diffractometer for crystal structure analysis
- Scanning electron microscope (SEM) for morphological analysis
- Fourier transform infrared spectroscopy (FTIR) for compositional analysis
- Brunauer Emmett Teller analysis (BET) for Surface area measurements
- Electrochemical Characterizations
- Cyclic Voltammetry (CV)
- Galvanostatic charge and discharge (GCD)

5.1 X-ray diffraction (XRD)

It is a rapid non destructive method employed for the measurement of crystal size (crystallinity) of compound equally applicable to liquid, powder, and crystals.

5.1.1 Instrumental principle

X-ray diffraction works on the principle of constructive interference of X-rays and crystalline material. It is used for the crystal structure determination of the material. It is a non-destructive technique, and it provides fingerprints of Bragg's reflections of crystalline materials [25, 26].

$$2d\sin\theta = n\lambda \dots\dots\dots (4)$$

This equation gives the information about the electromagnetic radiation's wavelength and the diffraction angle and their relationship to the lattice spacing in a crystalline material. Scanning at different 2θ angles is done due to the random orientation of particle diffraction in different directions is done. These diffraction peaks are studied for the identification of the crystalline

material because each crystalline material has its own set of particular d-spacing. This identification process is done by comparing d-spacing with some standard reference patterns.

5.1.2 Working

It consists of 3 main parts. A cathode tube, sample holder, and detector. X-rays are produced by heating filament element which accelerates electrons towards a target which collide with the target material with electrons. Crystal is composed of layers and planes “Diffraction” takes place, and it can be described as by Bragg’s Law. These reflections' positions tell us about inter-layer spacing-ray diffraction tells us about the phase, crystallinity, and sample purity. By this technique, one can also determine lattice mismatch, dislocations, and unit cell dimensions.

5.1.3 Crystal size measurement

Size measurement of particles is done using the Debye Scherer equation as

$$D = K\lambda/\beta\cos\theta \quad \dots\dots\dots 3$$

D= size of particle,K = shape factor, λ = wavelength of X-ray, β = full wave half width and θ is diffracted angel.

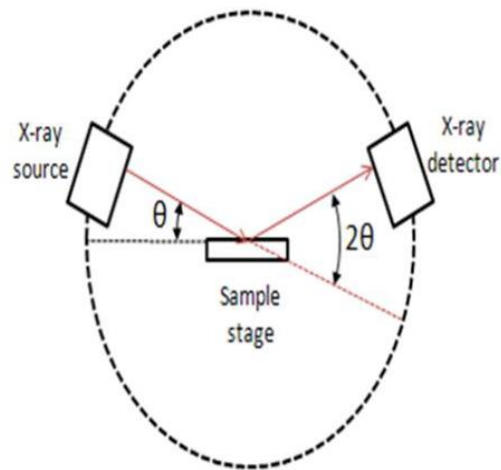
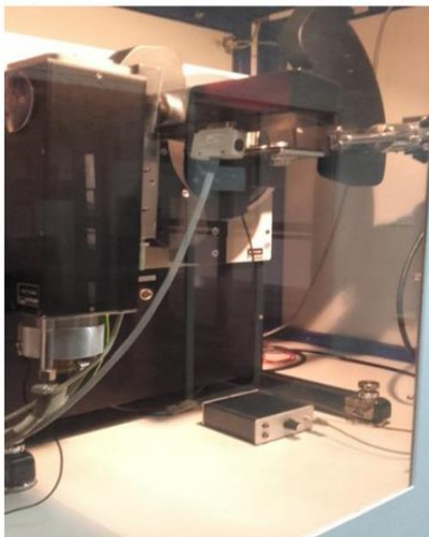


Figure 5.1 (a)XRD present at SCME NUST (b) Schematic of XRD

5.2 SEM Analysis

In this technique, the fine beam of electrons is focused over a specimen's surface. Photons or electrons are knocked off from the material's surface in the result. These knocked off electrons are then focused on the detector. The output from the detector modulates the brightness of the cathode ray tube (CRT). Every point where the electron beams are focused and interact, it is plotted on the consequent end on CRT, and the material's image is produced[27].

The electron-surface interaction causes the release of secondary electrons (SE), backscattered electrons (BSE), and X-rays[28]. Secondary electrons are used for detection. These electrons are emitted from the sample surface. So, a pronounced and clear image of the sample is obtained. It can reveal sample detail even less than 1nm in size. Also, the elastic scattering of incident electrons takes place and release backscattered electrons. They emerge from deeper locations as compared to secondary electrons. So, their resolution is comparatively low. When an inner shell electron knocks off from its shell, it emits characteristic x-rays [29]. We use SEM as it has easy sample preparation, and we can figure our sample's morphology, chemistry, crystallography, and orientation of planes. Magnification of SEM can be controlled from 10 to 500,000 times. Morphology of the materials was examined on (JEOL-JSM- 6490LA), and FESEM analysis were performed on (MIRA3 TESCAN). Elemental composition was determined by EDS detector attached to FESEM.

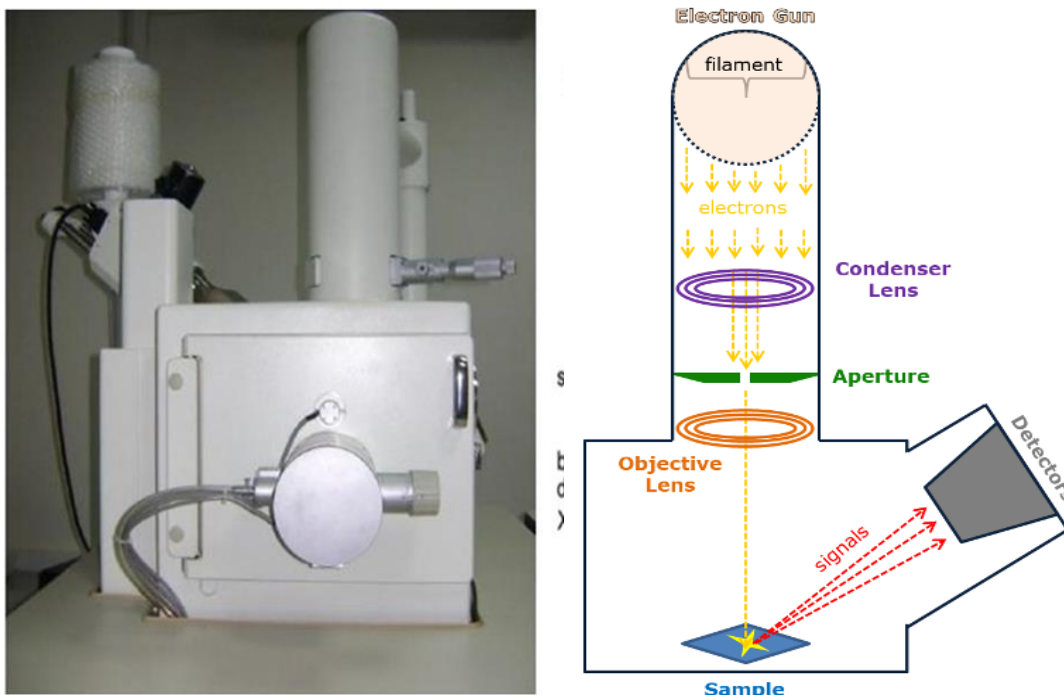


Figure 5.2 (a)JEOL-JSM- 6490LA Sem present at NUST SCME (b) Schematic of SEM

5.3 Brunauer Emmett Teller (BET)

Surface area and porosity are the vital property of a material which can be determined by BET analysis technique[30]. The equipment consists of several parts, sample preparation device, vacuum system, sample tube/Dewar, N₂ transfer system, computer hardware, and software. Working principle of BET is sample drying at elevated temperature with the purging of non-corrosive gases like N₂ then the amount of adsorbing N₂ is related to the specific surface area as well as pore volume. Sample preparation is a key step for BET analysis.[31]

First, the calculated amount of the sample is purified by degassing to remove the extra atmospheric contaminants like water vapours and air under elevated temperature for the desired amount of time under vacuum conditions in the sample preparation device. Then the sample test tube was placed in the surface area, and porosity analysis, which relates to the computing system and amount of adsorbing gases, is calculated, related to the surface area and total pore volume. BET analysis was performed at Gemini® VII 2390 instrument is present in SCME. The advantage of this equipment is accurate, fast, and simple to operate. Operating conditions were degassing of the sample at 300°C for 3 hrs. and analysis was performed at 0.05 to 0.3 p/p₀ range.



Figure 5.3 Gemini® VII 2390 Micro porosity analyzer

5.4 FTIR Analysis

FTIR analysis identifies various compounds, using infrared light to scan the sample and identify chemical bonds of a given sample. Using Alpha-FTIR spectrometer of Bruker Company, in the frequency range, 400-6000 cm^{-1} , identification of the synthesized sample is done.

5.4.1 Instrumentation

Transmission technique is employed for FTIR analysis light is focused on sample that is inserted into optical path length, the light that is directed over sample at different angles cause the phenomenon of internal reflection and then bounces back from top and bottom of the crystal. Energy interactions occur between the interface of the sample and crystal, and the bounce position is located. More energy transfer occurs where large bounce takes place.

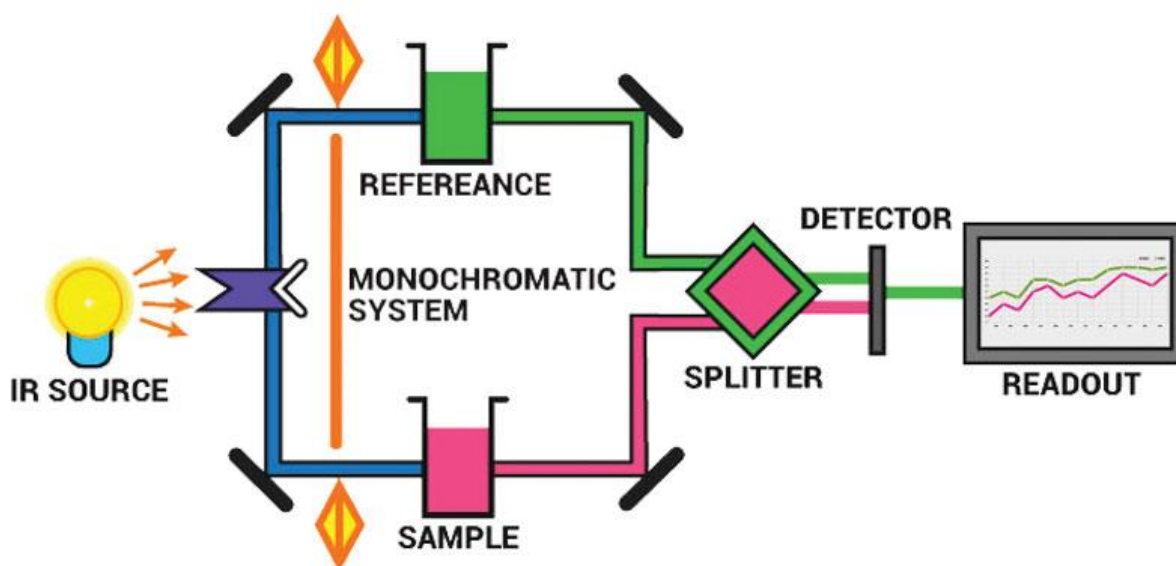


Figure 5.4 Working of FTIR

5.5 Electrochemical Workstation

Biologic VSP is the research-grade potential stat present at SCME. The equipment consists of workstation, electrochemical cell, computer hardware, and software system. It is used for many applications, including

- Battery testing

- Fuel cell and biofuel cell
- Liquid conductivity
- Electrochemical deposition of thin film
- Material impedance spectroscopy
- Corrosion testing
- Photovoltaics and sensors
- Capacitor and supercapacitor testing

5.5.1 Supercapacitor performance testing

The testing of supercapacitor material can be checked in two ways, i-e, two electrodes or three-electrode cell configurations. The three-electrode assembly enables the measurements of electrochemical reactions, which are occurring at one electrode, and this electrode under study is called the working electrode (WE). Another electrode called a counter electrode (CE) completes the electrochemical circuit, while the reference electrode (RE) gives a constant reference point for the potential measurements. A potential state measures the current flow between WE and CE, and the potential difference between WE and RE. The electrochemical workstation was used for the electrochemical performance of the electrode material. Three electrode system is employed using glassy carbon with 0.0707 cm^2 area coated with 0.1mg of different composite material as working electrode, calomel electrode ($\text{Hg}/\text{Hg}_2\text{SO}_4$) as reference one, and Pt wire as a counter electrode. All the cyclic voltammetry performance done in this work was carried out within the potential window from -0.1 to 0.9 V in 1MKOH as the electrolyte.



Figure 5.5 Biologic VSP Electrochemical Workstation

5.5.2 Electrode preparation

For performing cyclic voltammetry, Glassy carbon electrode(GCE) was used as a working electrode. This GCE was modified with our synthesized material. In this modification process, 1mg of active material, 100 μ L DMF, and 5 μ L Nafion were sonicated for 20 minutes, and then 10 μ L was drp cast on GCE and then dried. This was used as modified.



Figure 5.6 Electrode Modification

5.6 Cyclic Voltammetry

It is the simplest method in laboratory scale to measure the electrochemical behavior. Oxidation and reduction can be analyzed by CV, which occurs at the electrode/electrolyte interface. The cyclic Voltammetry system consists of the working electrode (WE), a reference electrode (RE), and the counter electrode (CE). In CV, the potential is charged on the WE and RE, and the resulting output current response is recorded between the working and counter electrode. CV curve is the resulting current(I) of WE vs. the potential (V). Potential is applied between the WE and RE. The most commonly used RE are saturated calomel electrode (SCE) and Silver/Silver chloride (Ag/AgCl). The counter electrode is mostly Platinum. The purpose of the electrolyte is to provide ions. The electrolyte must possess good conductivity. In supercapacitors, different materials show different responses. EDLC gives a rectangular curve, whereas the pseudo capacitor gives oxidation and reduction hump during forwarding, and a reverse scan shows redox occurs in Fig.

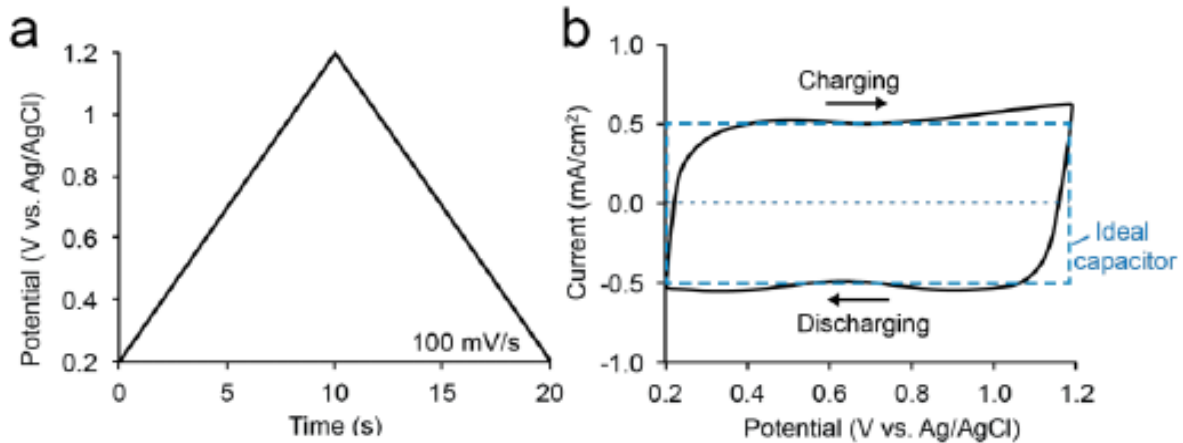


Figure 5.7 a) Applied voltage with time b) Ideal voltammogram

5.7 Galvanostatic Charge Discharge

GCD is the most common method to test the charging and discharging of the supercapacitors and batteries. GCD measure the potential with time at constant current. One charge and discharge of the material is equal to one complete cycle. Similar to CV, the GCD curves of EDLC and Pseudo capacitor is different. EDLC materials In EDLC type supercapacitors, the charge-discharge cycles show linear curves with very little IR drop.

In contrast, in the case of Pseudo capacitors, the curve is not linear, and the IR drop is large compared to the EDLC. This deviation refers to the charge storage mechanism, which takes place due to the oxidation and reduction reactions. Similarly, the linear response shows that the charge storage mechanism is not faradaic, means that only physical charge storage occurs. GCD curves of both EDLC and Psuedo capacitor in the figure above part a.

5.8 Cyclic Stability

Cyclic stability is one of the essential parameters of energy storage devices. The cyclic performance of supercapacitors is tested by multiple charge-discharge cycles. On a lab-scale, normally 500 to 10000 charge-discharge cycles were conducted to examine the capacitance retention of the material.

Chapter No 6

Results and discussions

This chapter illustrates the results, the obtained data from therein, and their interpretation in the context of set objectives and hypotheses of the work.

6.1 Xrd analysis

This analysis was carried out to examine the crystal structure of the sample. This analysis confirms the presence of nickel and manganese ion in composite material. X-ray diffraction (XRD) was carried out using Stove diffractometer at Scme Nust operating voltage of 40 kV and a current of 40 mA with Cu $K\alpha$ radiation. The XRD patterns of pure manganese oxide and Nickel doped manganese oxide is shown in Fig.6.1. The main peak detected for manganese oxide (MnO_2), which shows the prominent diffraction peaks of pure nanowires of MnO_2 at 2 θ at 12.784, 18.10, 28.84, 37.52, 41.969, 49.86 correspondings to (110) (200) (310) (211) (301) and (411) planes which index the tetragonal structure of MnO_2 (JCPDS card no 00-044-0141) as shown in Fig 6.1. The XRD patterns of Ni-doped MnO_2 were the same, as shown in Fig.6.1. The diffraction pattern was observed at 18.891, 29.884, 35.197, 42.771, 56.514, 62.086 correspondings to at (111), (220), (311), (400), (511), (440) planes, which index the cubic structure of NMO regarding JCPDS card no. (01-084-0542). The sharp and narrow peaks of Ni-doped manganese oxide represents that they are highly crystalline. The improved crystallinity is shown by the peak intensity. It proves that the addition of nickel facilitates the formation of MnO_2 . The manganese oxide present in many crystallographic forms, such as 1D,2D,3D structure. The position of atoms in the unit cell affect the intensities but not the directions of diffracted beams. The crystal size was calculated using

$$D = 0.9\lambda / (\beta \cos\theta) \dots\dots\dots 4$$

Where θ is the angle of the diffracted peak, B is FWHM, and λ is the wavelength.

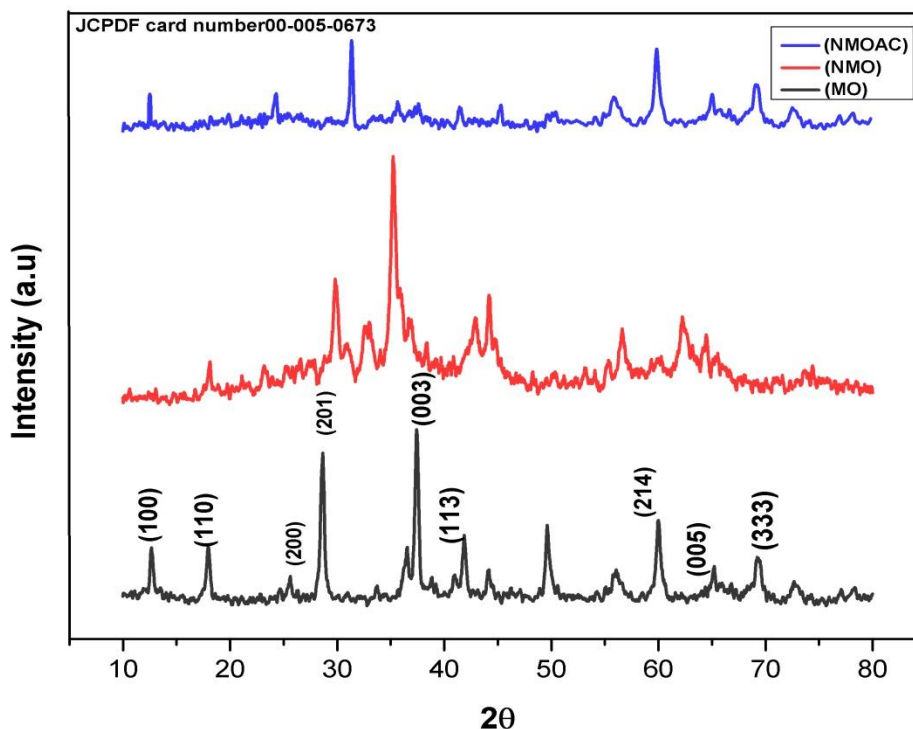


Figure 6.1 XRD of Nickel manganese oxide with Activated Carbon nanocomposites.

6.2 FTIR Analysis

The result of FTIR spectra served as evidence to check the presence and formation of single manganese oxide and nickel doped manganese oxide in a sample. The IR bands of inorganic products are due to the vibrations of ions in the crystal lattices. The peaks observed in the range of 375 cm^{-1} to 1000 cm^{-1} are due to the metal-oxide bands. This confirms the existence of single and mixed oxide bands. The absorption of highest band generally for all metal oxide bands are observed in the range of 600 to 550 cm^{-1} which shows the stretching vibrations of atoms. The lowest bands are in the range of 450 to 385 cm^{-1} . The intense band is observed at 527 cm^{-1} due to Ni-O band. The band observed in the range of 714.16 cm^{-1} shows the distortion of Mn-O band. The nickel doped manganese oxide shows in fig 6.3. This spectrum confirms the presence of metal oxide. These results are in good agreement in published literature. [32, 33]

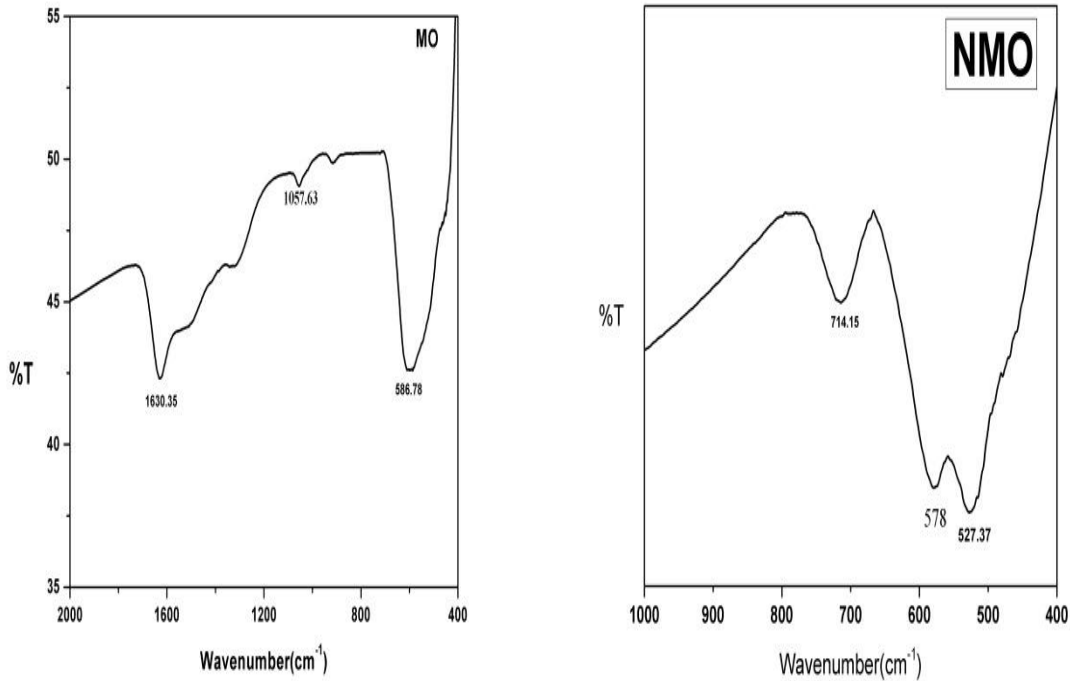


Figure 6.2 FTIR spectra of Nickel Manganese Oxide

6.3 SEM Analysis

This characterization technique was carried out on a Geol 3800 operated at 10 kV. Sem analysis is used for morphology detection. Fig.6.4 shows the formation of MnO₂ and NMO nanowires successfully. This analysis of NMO shows the hierarchical nanostructures. Nanowires are arranged in one direction, which shows the porous nature of the material and good transport of electrolyte during an electrochemical performance. The flower-like structure is clearly shown in Fig 6.4(b). Figure 6.4a-b shows the SEM image for as prepared α -MnO₂. The products consist of nanowires with diameters about 1-100nm and length ranging between 1 μ m and 10 μ m[34].it illustrates the single crystalline nature of the α -MnO₂ nanowire, although some crystal defects can be observed on the surface of the nanowire. This structure shows the rapid ion transport mechanism, which increases the electrochemical properties of the material.[34]

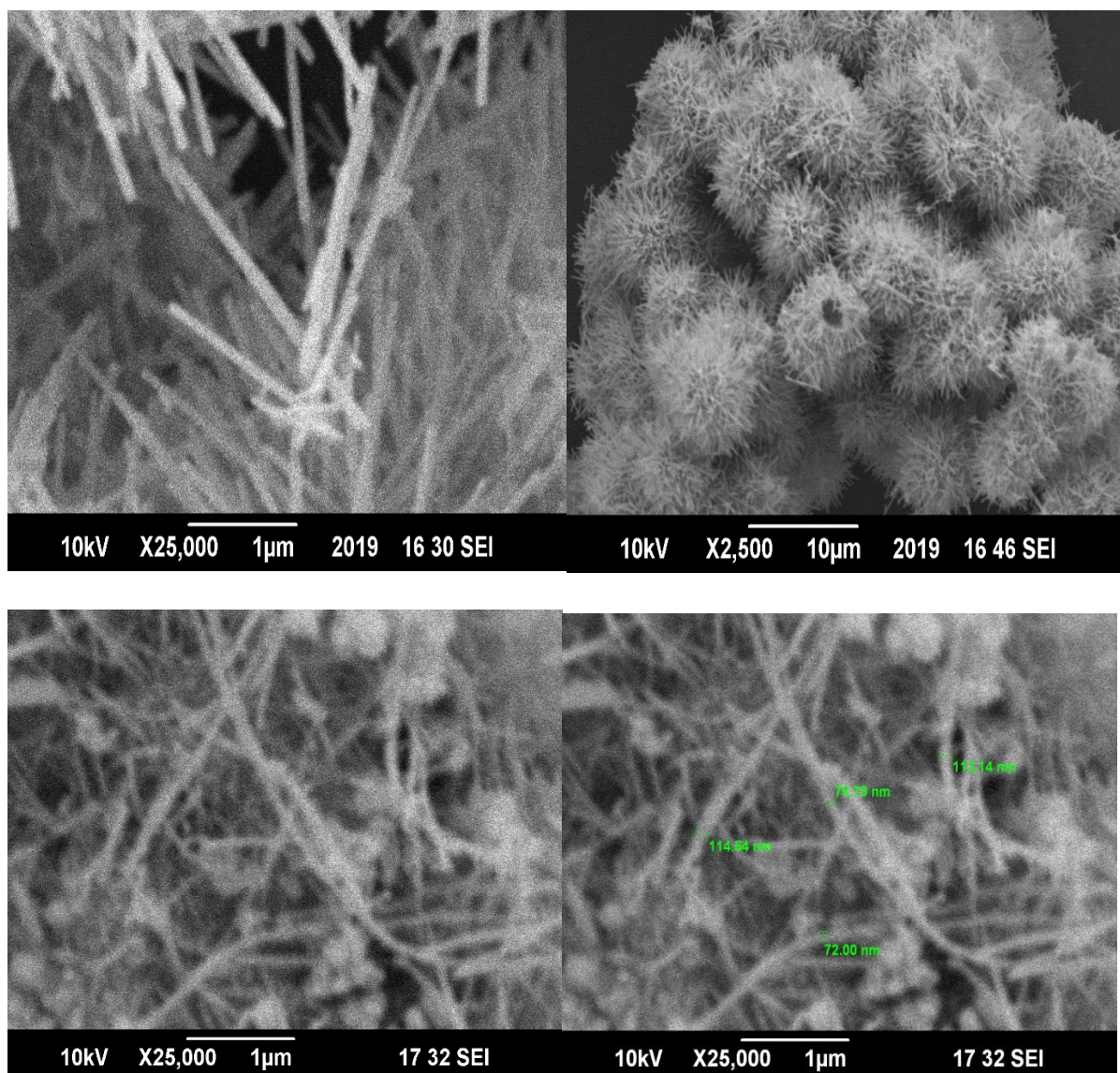


Figure 6.3 SEM analysis of MO/NMO/NMOAC

6.4 Electrochemical properties analysis

6.4.1 Cyclic voltammetry of MO

Cyclic voltammetry was performed to check the faradaic response at various scan rates (25, 50, 100mV/s) using a glassy carbon electrode and nafion as a binder in 1 M KOH electrolytes. The non-rectangular shape confirms the faradaic redox reaction and the pseudocapacitive nature of MO, NMO, NMOAC electrode material. The potential windows are from 0.1 to 0.6. The cyclic voltammetry shows three pairs of characteristic peaks due to the redox reactions. It can be seen from figure 6.4 that the prepared electrode materials have better charge ad discharge

reversible capacitance characteristics. The specific capacitances of samples are calculated from CV curves using the following equation.

$$C_s = \frac{\int idV}{mv \Delta V} \text{-----} 5$$

Where

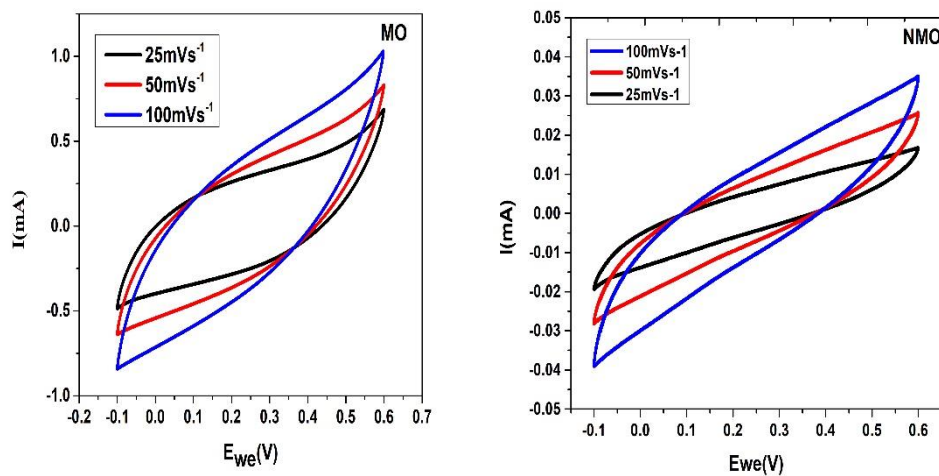
‘Cs’ is the specific capacitance

‘I’ is the current response density,

‘m’ is the mass of the active material, which is 1mg

‘v’ is the scan rate, and ΔV is the potential window of discharge.

Specific capacitance decrease with the increasing scan rate due to limited faradaic redox reaction as less active sites available as compared to the lowest scan rate at which highest capacitance due to more redox-active sites.[35]This occurs dur to because at low scan rate ions have maximum time for interclation,while at igh scan rateions have less time that’s why specific capacitance becomes grater at lower scan rate. The specific capacitance of MO is 556.661 F/g, NMO is 1614.11 F/g, and NMOAC is 1347.609 F/g .The addition of MnO2 improved the electrochemical performance of activated carbon, the excess porosity of MnO2 will cause a decrease of porosity, which will cause a decrease of the electrochemical performance of composites. The optimal ratio of composite is 1:1 (weight ratio).This leads to decrease the specific capacitance.[36]This shows that the incorporation of nickel ion in the lattice of manganese oxide improves the electrochemical performance of the material. The following graphs shown in t at different scan rates are shown in fig.6.5.



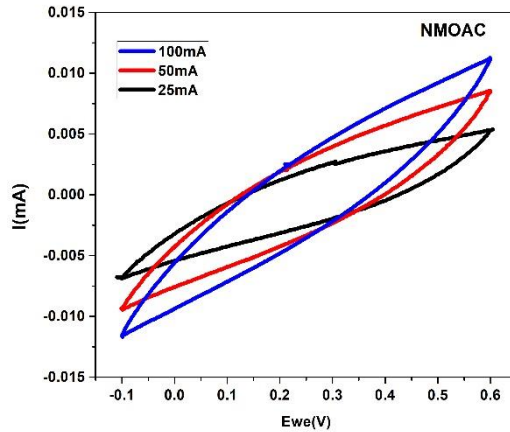


Figure 6.4 (a)CV of the MO (b) CV of NMO materials (c)CV of NMOAC

The C_s of the nickel manganese oxide and composite material is relatively larger. The manganese dioxide lattice will expand due to the incorporation of nickel element, which facilitates rapid insertion and extraction of electrolyte ions in the electrode materials, due to improving the specific capacitance of the electrode materials.

6.4.2 Galvanostatic Charge discharge

The galvanostatic charge-discharge analysis was performed on the workstation at different current densities. The capacitive performance was analyzed. Figure 6.6 shows GCD curves of MO and NMO at 3A g⁻¹, 6 A g⁻¹, 8A g⁻¹, and 12A g⁻¹ with an operating window of -0.1 V to 0.5 V. The charges storage mechanism is due to oxidation and reduction. It is evident from the curves that NMO exhibits longer discharge time than MO, and pure oxides demonstrate that the electrochemical performance of NMO was far superior due to the doping of nickel cations. GCD is the most accurate way to calculate specific capacitance. Specific capacitance is calculated by

$$C_s = \frac{I \cdot t}{m \cdot \Delta V} \text{-----6}$$

Here, “t” is discharge time

“I” represents current density and “m” is mass of active material

ΔV is the voltage drop during discharge.

The GCD is a more accurate way to find the specific capacitance. NMO shows good specific capacitance of 374.4 F g^{-1} , 810 F g^{-1} , 1104 F g^{-1} , 1634.4 F g^{-1} at 3 Ag^{-1} , 6 Ag^{-1} , 8 Ag^{-1} and 12 Ag^{-1} as shown in table.

6.5 Energy Density and Power Density

The energy density and power density also calculated using the following relation.

Energy density and power density was calculated by

$$\text{Energy Density(ED)} = \frac{1}{2} C_s \Delta V^2 \text{-----7}$$

$$\text{Power Density(PD)} = \frac{ED}{\Delta t} \text{-----8}$$

Here, C_s is the specific capacitance calculated from CV or GCD, and ΔV is the operating voltage, and Δt is discharge time.

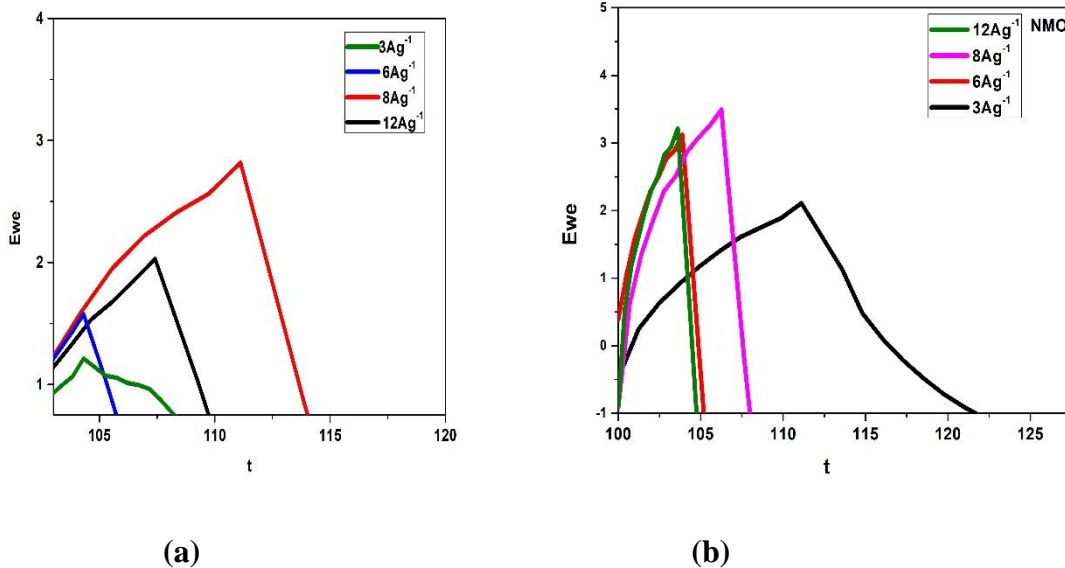
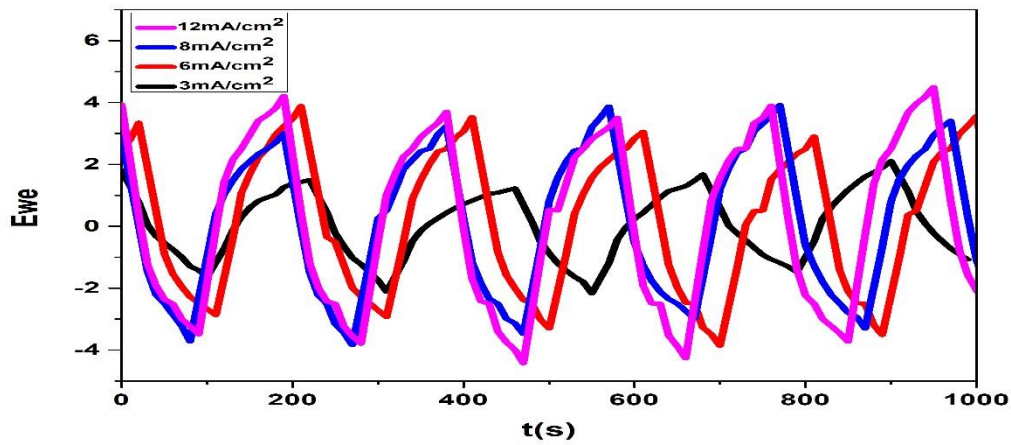


Figure 6.5 (a) Charge and discharge curves of sample MO at different current densities, (b) Charge and discharge curves of sample NMO at different current densities.

Moreover, MO and NMOAC exhibit less performance as compared to NMO, as represented in Table. NMO shows excellent energy density and power density of 294.192 Wh kg⁻¹ and 1.294W kg⁻¹ at 12A g⁻¹.



(a)

Figure 6.6 (a) Charge and discharge curves at different densities

6.6 Cyclic Stability

It is one of the prominent feature of electrode material to utilize these materials for practical applications. The stability of these synthesized samples was investigated by using charge discharge method at the current density of 1mA/cm²for 10000 cycles as illustrated in Figure 6.7. It is evident from results that specific capacitance is relatively unstable during first few hundred cycles, It is due to electrode material is unstable because of pre activation processes. The electrode material anomalous behaviours corroborated the effects of pre activation performs the effect of capacitance retentions.

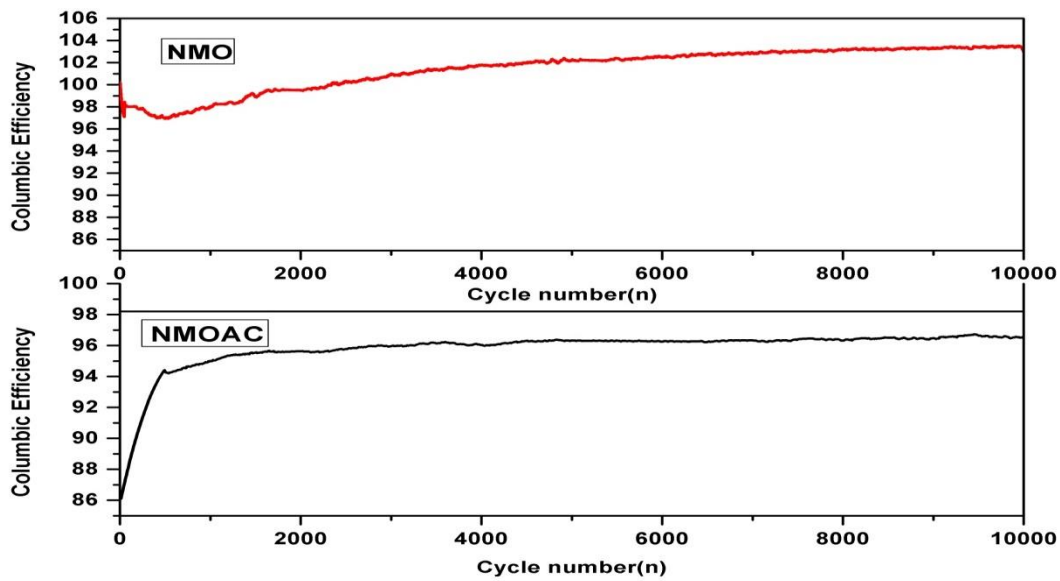


Figure 6.7 Long-term cycling stability of sample MO and NMO

	MO		NMO		NMO/AC	
Current density	Specific capacitance	Current density	Specific capacitance	Current density	Specific capacitance	
(Ag ⁻¹)	(Fg ⁻¹)	(Ag ⁻¹)	(Fg ⁻¹)	(Ag ⁻¹)	(Fg ⁻¹)	
3	68.4	3	374.4	3	419.9	
6	144	6	810	6	775.3834	
8	201.6	8	1104	8	960	
12	324	12	1634.4	12	1384.61	

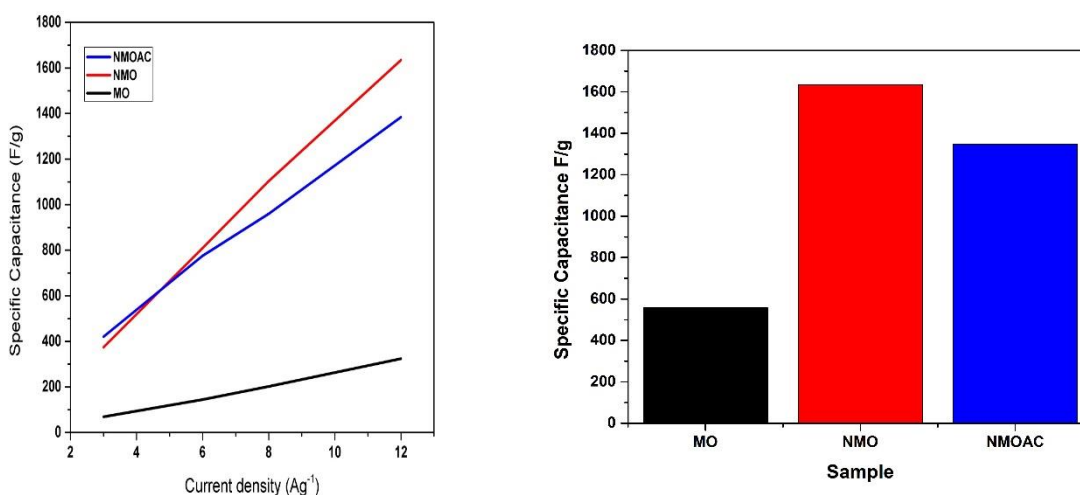


Figure 6.8 (a) Specific Capacitance of MO, NMO, NMOAC different current densities (b) Comparison of capacitance

6.7 Raman Spectroscopy

An examination of Raman spectroscopy has also been used to confirm nickel and manganese ions in the sample. Figure 6.10 shows the Raman spectra of MO, NMO, and NMOAC samples. MnO₂ thin film vibrational mode at 508 cm⁻¹, 651 cm⁻¹ corresponds to the stretching behavior of the MnO₆ octahedral. The corresponding antisymmetry stretching bands are obtained in the infrared spectrum at 144 cm⁻¹ and 293.01 cm⁻¹. The low-intensity Raman bands explained the deformation modes of the metal-oxygen chain of Mn–O–Mn in the MnO₂ octahedral lattice. The Ni doped MnO₂ sample exhibited Raman vibration bands similarly. Also, the vibration peaks at lower wavenumber were slightly shifted, as shown in Fig 6.10. The results showed that the presence of Ni ion affected the local structure of MnO₂, typically the short-range environment of oxygen coordination around transition metal cations in MnO₂ lattice.

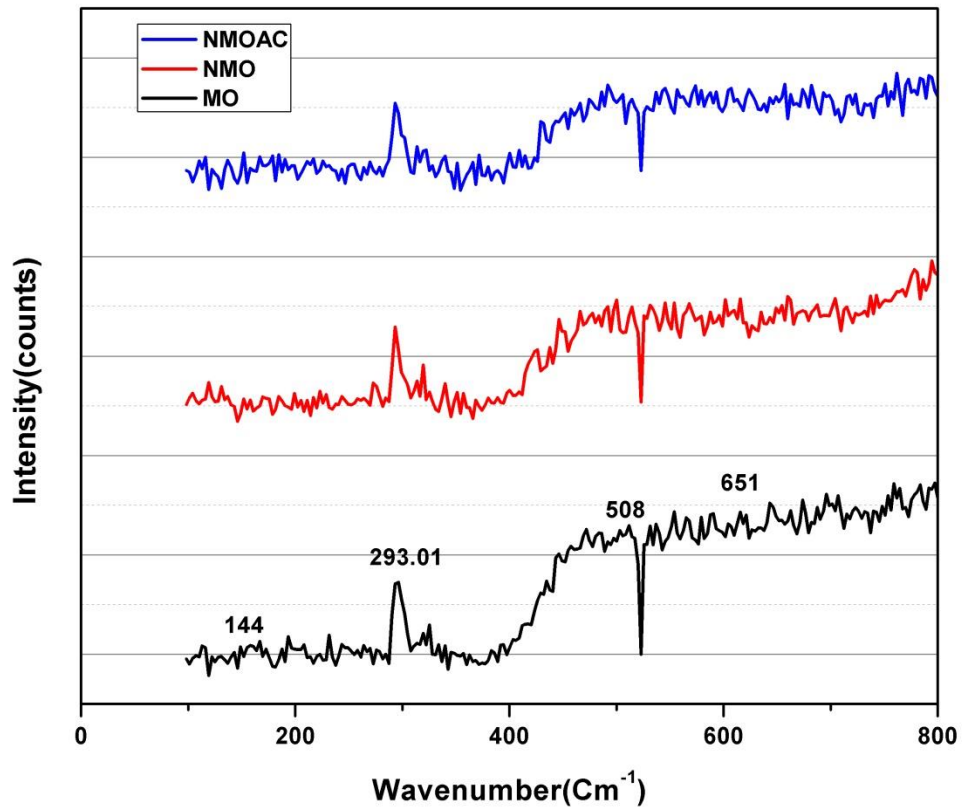


Figure 6.9 Raman spectra of Manganese Oxide and Ni-doped Manganese oxide

Conclusion

In this work, we investigated the in situ inclusion of nickel in manganese oxide lattice and tested the composite material as supercapacitor electrodes. MO nanowires of a hierarchical mesoporous structure were successfully synthesized. The excellent capacitance of 1636.4Fg^{-1} was achieved as well as it gives remarkable cyclic stability with capacitance retention of 95.5% up to 5,000 GCD cycles proves NMO as potential candidate for the electrode material for energy storage devices. Furthermore, the superior electrochemical performance of NMO/AC illustrates that it will meet the modern-day energy applications demand and one of the desired materials for supercapacitors for flexible electronics.

References

- [1]. C. Garino, L. J. P. T. o. t. R. S. A. M. Salassa, Physical, and E. Sciences, "The photochemistry of transition metal complexes using density functional theory," vol. 371, no. 1995, pp. 20120134, **2013**.
- [2]. Y. Zhu, S. Murali, M. D. Stoller, K. Ganesh, W. Cai, P. J. Ferreira, A. Pirkle, R. M. Wallace, K. A. Cychoz, and M. J. s. Thommes, "Carbon-based supercapacitors produced by activation of graphene," vol. 332, no. 6037, pp. 1537-1541, **2011**.
- [3]. A. Dehghani-Sanij, E. Tharumalingam, M. Dusseault, R. J. R. Fraser, and S. E. Reviews, "Study of energy storage systems and environmental challenges of batteries," vol. 104, pp. 192-208, **2019**.
- [4]. E. E. Miller, Y. Hua, and F. H. J. J. o. E. S. Tezel, "Materials for energy storage: Review of electrode materials and methods of increasing capacitance for supercapacitors," vol. 20, pp. 30-40, **2018**.
- [5]. J. Xu, L. Gao, J. Cao, W. Wang, and Z. J. E. A. Chen, "Preparation and electrochemical capacitance of cobalt oxide (Co₃O₄) nanotubes as supercapacitor material," vol. 56, no. 2, pp. 732-736, **2010**.
- [6]. J. Mei, T. Liao, G. A. Ayoko, J. Bell, and Z. J. P. i. M. S. Sun, "Cobalt oxide-based nanoarchitectures for electrochemical energy applications," vol. 103, pp. 596-677, **2019**.
- [7]. G. Z. J. I. M. R. Chen, "Supercapacitor and supercapattery as emerging electrochemical energy stores," vol. 62, no. 4, pp. 173-202, **2017**.
- [8]. H. Wang, J. Lin, Z. X. J. J. o. s. A. m. Shen, and devices, "Polyaniline (PANi) based electrode materials for energy storage and conversion," vol. 1, no. 3, pp. 225-255, **2016**.
- [9]. A. Eftekhari, L. Li, and Y. J. J. o. P. S. Yang, "Polyaniline supercapacitors," vol. 347, pp. 86-107, **2017**.
- [10]. M. S. Kumar, K. Y. Yasoda, S. K. Batabyal, and N. K. J. M. R. E. Kothurkar, "Carbon-polyaniline nanocomposites as supercapacitor materials," vol. 5, no. 4, pp. 045505, **2018**.
- [11]. S.-Y. Lee, J.-I. Kim, and S.-J. J. E. Park, "Activated carbon nanotubes/polyaniline composites as supercapacitor electrodes," vol. 78, pp. 298-303, **2014**.

- [12]. S. K. Kandasamy, K. J. J. o. I. Kandasamy, O. Polymers, and Materials, "Recent advances in electrochemical performances of graphene composite (graphene-polyaniline/polypyrrole/activated carbon/carbon nanotube) electrode materials for supercapacitor: A review," vol. 28, no. 3, pp. 559-584, **2018**.
- [13]. Y. Huang, H. Li, Z. Wang, M. Zhu, Z. Pei, Q. Xue, Y. Huang, and C. J. N. E. Zhi, "Nanostructured polypyrrole as a flexible electrode material of supercapacitor," vol. 22, pp. 422-438, **2016**.
- [14]. W. K. Chee, H. N. Lim, and N. M. J. I. J. o. E. R. Huang, "Electrochemical properties of free-standing polypyrrole/graphene oxide/zinc oxide flexible supercapacitor," vol. 39, no. 1, pp. 111-119, **2015**.
- [15]. P. Poizot, S. Laruelle, S. Grugeon, L. Dupont, and J. J. N. Tarascon, "Nano-sized transition-metal oxides as negative-electrode materials for lithium-ion batteries," vol. 407, no. 6803, pp. 496-499, **2000**.
- [16]. M. Chhowalla, H. S. Shin, G. Eda, L.-J. Li, K. P. Loh, and H. J. N. c. Zhang, "The chemistry of two-dimensional layered transition metal dichalcogenide nanosheets," vol. 5, no. 4, pp. 263-275, **2013**.
- [17]. A. Matnishyan, T. Akhnazaryan, G. Abagyan, G. Badalyan, S. Petrosyan, and V. J. P. o. t. S. S. Kravtsova, "Synthesis and study of polyaniline nanocomposites with metal oxides," vol. 53, no. 8, pp. 1727, **2011**.
- [18]. D. M. Alqahtani, C. Zequine, C. Ranaweera, K. Siam, P. K. Kahol, T. P. Poudel, S. Mishra, R. K. J. J. o. A. Gupta, and Compounds, "Effect of metal ion substitution on electrochemical properties of cobalt oxide," vol. 771, pp. 951-959, **2019**.
- [19]. T. Matsunaga, R. Tomoda, T. Nakajima, and H. J. F. M. 1. Wake, "Photoelectrochemical sterilization of microbial cells by semiconductor powders," vol. 29, no. 1-2, pp. 211-214, **1985**.
- [20]. X. Tong, E. Ashalley, F. Lin, H. Li, and Z. M. J. N.-M. L. Wang, "Advances in MoS₂-based field effect transistors (FETs)," vol. 7, no. 3, pp. 203-218, **2015**.
- [21]. H. Li, J. Wu, Z. Yin, and H. J. A. o. c. r. Zhang, "Preparation and applications of mechanically exfoliated single-layer and multilayer MoS₂ and WSe₂ nanosheets," vol. 47, no. 4, pp. 1067-1075, **2014**.

- [22]. J. Shen, Y. He, J. Wu, C. Gao, K. Keyshar, X. Zhang, Y. Yang, M. Ye, R. Vajtai, and J. J. N. I. Lou, "Liquid phase exfoliation of two-dimensional materials by directly probing and matching surface tension components," vol. 15, no. 8, pp. 5449-5454, **2015**.
- [23]. S. A. Ansari, R. Kumar, M. Barakat, and M. H. J. J. o. M. S. M. i. E. Cho, "Simple and sustainable route for large scale fabrication of few layered molybdenum disulfide sheets towards superior adsorption of the hazardous organic pollutant," vol. 29, no. 9, pp. 7792-7800, **2018**.
- [24]. G. Cunningham, M. Lotya, C. S. Cucinotta, S. Sanvito, S. D. Bergin, R. Menzel, M. S. Shaffer, and J. N. J. A. n. Coleman, "Solvent exfoliation of transition metal dichalcogenides: dispersibility of exfoliated nanosheets varies only weakly between compounds," vol. 6, no. 4, pp. 3468-3480, **2012**.
- [25]. N. Hossain, "Synthesis and Characterization of NbO_x Thin Film," University of Saskatchewan, **2019**.
- [26]. H. Stanjek, and W. J. H. I. Häusler, "Introduction To Powder/Polycrystalline Diffraction," vol. 154, pp. 107-119, **2004**.
- [27]. R. R. R. U. m. V. a. c. s. u. P. U. S. e. m. s. o. m. c. i. c. s. u. m. w. p. Jerosch J.
- [28]. C. J. J. o. A. P. Oatley, "The early history of the scanning electron microscope," vol. 53, no. 2, pp. R1-R13, **1982**.
- [29]. S. Chatti, L. Laperrière, G. Reinhart, and T. Tolio, CIRP encyclopedia of production engineering: Springer Berlin Heidelberg, **2019**.
- [30]. M. Naderi, "Surface Area: Brunauer–Emmett–Teller (BET)," Progress in filtration and separation, pp. 585-608: Elsevier, 2015.
- [31]. J. Hao, Y. Liu, H. Shen, W. Li, J. Li, Y. Li, and Q. J. J. o. M. S. M. i. E. Chen, "Effect of nickel-ion doping in MnO₂ nanoneedles as electrocatalyst for the oxygen reduction reaction," vol. 27, no. 6, pp. 6598-6605, **2016**.
- [32]. P. W. Menezes, A. Indra, O. Levy, K. Kailasam, V. Gutkin, J. Pfrommer, and M. Driess, "Using nickel manganese oxide catalysts for efficient water oxidation," Chemical Communications, vol. 51, no. 24, pp. 5005-5008, **2015**.

- [33]. M. Zhang, S. Guo, L. Zheng, G. Zhang, Z. Hao, L. Kang, and Z.-H. J. E. a. Liu, "Preparation of NiMn₂O₄ with large specific surface area from an epoxide-driven sol-gel process and its capacitance," vol. 87, pp. 546-553, **2013**.
- [34]. J. Fei, Y. Cui, X. Yan, W. Qi, Y. Yang, K. Wang, Q. He, and J. J. A. M. Li, "Controlled preparation of MnO₂ hierarchical hollow nanostructures and their application in water treatment," vol. 20, no. 3, pp. 452-456, **2008**.
- [35]. T.-W. Kim, S.-J. J. J. o. C. Park, and I. Science, "Synthesis of reduced graphene oxide/thorn-like titanium dioxide nanofiber aerogels with enhanced electrochemical performance for supercapacitor," vol. 486, pp. 287-295, **2017**.
- [36]. J. R. Choi, J. W. Lee, G. Yang, Y.-J. Heo, and S.-J. J. C. Park, "Activated Carbon/MnO₂ Composites as Electrode for High Performance Supercapacitors," vol. 10, no. 2, pp. 256, **2020**.